RM-315

POLARIMETRIC MEASUREMENTS OF SIMULATED LUNAR SURFACES (PHASE III)

March 1966

GPO PRICE $ _____

CFSTI PRICE(S) $ _____

Hard copy (HC) 2.50

Microfiche (MF) .75

ff 653 July 65

Grumman

RESEARCH DEPARTMENT

FACILITY FORM 602

N66 35959 (ACCESSION NUMBER)

(THRU)

75 (PAGES)

1 (CODE)

CR-77764 (NASA CR OR TMX OR AD NUMBER)

30 (CATEGORY)

GRUMMAN AIRCRAFT ENGINEERING CORPORATION

BETHPAGE NEW YORK

Grumman Research Department Memorandum RM-315

POLARIMETRIC MEASUREMENTS OF SIMULATED LUNAR SURFACES

PHASE III

by

W. G. Egan

and

L. L. Smith

Geo-Astrophysics Section

March 1966

Third Interim Report on Contract NAS 9-4942

Approved by: Charles E. Mack, Jr.
Charles E. Mack, Jr.
Director of Research

ACKNOWLEDGMENTS

The authors wish to acknowledge the continuing efforts of H. B. Hallock, J. Grusauskas and D. R. Lamberty in perfecting the polarimetric analyzer and recording data. We wish also to give thanks to C. Bartollota, C. Krolik, and D. Schlaijker, for their assistance.

We are also grateful to the following individuals for discussions in relation to the pursuit of the program: J. Halajian, Dr. G. McCoyd, Dr. N. Milford, J. Reichman, Dr. M. Sidran, and F. Spagnolo.

TABLE OF CONTENTS

Item	Page
Introduction and Summary	1
Test Equipment	3
Description	3
Source Polarization	3
Calibration	3
Standard Polarimetric Curves and Data Presentation	5
Phase III — Contrived Models	7
Purpose	7
Test Specimens and Sample Preparation	7
Experiments	9
Discussion of Results	9
Lunar Implications	19
Conclusions	21
Recommendations	22
References	23

LIST OF ILLUSTRATIONS

Figure		Page
1	Polarization Curves of the Moon -- Ultraviolet Range, 0.36μ (Gehrels et al.)	25
2	Polarization Curves of the Moon -- Green Range, 0.54μ (Gehrels et al.)	26
3	Polarization Curves of the Moon -- Infrared Range, 0.94μ (Gehrels et al.)	27
4	Contrived Model No. 1 Development	28
5	Contrived Model No. 2 Development	29
6	Contrived Model No. 4 Development	30
7	Contrived Model No. 5 Development	31
8	Contrived Model No. 6 Development	32
9	Contrived Model No. 7 Development	33
10	Contrived Model No. 1: Furnace Slag (Spongelike-NASA) Topped with 0.088 to 0.21 mm Particles of Volcanic Ash No. 1	34
11	Contrived Model No. 1: Percent Polarization as a Function of Color -- 60° Polarimeter	35
12	Contrived Model No. 1: Simulated Lunar Longitude Effect on Percent Polarization as a Function of Color	36
13	Contrived Model No. 2: Coral No. 1 Topped with Particles of Furnace Slag No. 4 $\leq$ 0.037 mm	37
14	Contrived Model No. 2: Percent Polarization as a Function of Color -- 60° Polarimeter	38
15	Contrived Model No. 2: Simulated Lunar Longitude Effect on Percent Polarization as a Function of Color	39

Figure		Page

16 Contrived Model No. 4: Volcanic Ash No. 4 (Chunks) Topped with Particles of Coral $\leq 1\mu$ 40

17 Contrived Model No. 4: Percent Polarization as a Function of Color -- 60° Polarimeter 41

18 Contrived Model No. 4: Simulated Lunar Longitude Effect on Percent Polarization as a Function of Color 42

19 Contrived Model No. 5: Volcanic Ash No. 4 Topped with Particles of Itself $\leq 1\mu$ 43

20 Contrived Model No. 5: Percent Polarization as a Function of Color -- 60° Polarimeter 44

21 Contrived Model No. 5: Simulated Lunar Longitude Effect on Percent Polarization as a Function of Color 45

22 Contrived Model No. 6: Volcanic Ash No. 1 Topped with Particles of Itself $\leq 1\mu$ 46

23 Contrived Model No. 6: Percent Polarization as a Function of Color -- 60° Polarimeter 47

24 Contrived Model No. 6: Simulated Lunar Longitude Effect on Percent Polarization as a Function of Color 48

25 Contrived Model No. 7: Furnace Slag No. 4 (2.83-6.35mm) Topped with Particles of Itself $\leq 1\mu$ 49

26 Contrived Model No. 7: Percent Polarization as a Function of Color -- 60° Polarimeter 50

27 Contrived Model No. 7: Simulated Lunar Longitude Effect on Percent Polarization as a Function of Color 51

28 Comparison of Maximum Percent Polarization as a Function of $1/\lambda$ 52

Figure		Page

29 Comparison of Normal Albedos as a Function of $1/\lambda$ ... 53

30 Comparison of Inversion Angles as a Function of $1/\lambda$ 54

31 Comparison of Maximum Percent Polarization as a Function of Normal Albedo 55

32 Comparison of Maximum Percent Polarization and Corresponding Phase Angle 56

33 Photometry of Contrived Model No. 1: Furnace Slag (Spongelike-NASA) Topped with 0.088 to 0.21 mm Particles of Volcanic Ash No. 1 (Brightness (Arbitrary Units) versus Phase Angle) ... 57

34 Photometry of Contrived Model No. 2: Coral No. 1 Topped with Particles of Furnace Slag No. 4 $\leq$ 0.037 mm (Brightness (Arbitrary Units) versus Phase Angle) 58

35 Photometry of Contrived Model No. 4: Volcanic Ash No. 4 (Chunks) Topped with Particles of Coral $\leq 1\mu$ -- 60° Photometer-Visual Light (Brightness (Arbitrary Units) versus Phase Angle) ... 59

36 Photometry of Contrived Model No. 5: Volcanic Ash No. 4 Topped with Particles of Itself $\leq 1\mu$ (Brightness (Arbitrary Units) versus Phase Angle) ... 59

37 Photometry of Contrived Model No. 6: Volcanic Ash No. 1 Topped with Particles of Itself $\leq 1\mu$ (Brightness (Arbitrary Units) versus Phase Angle) ... 60

38 Photometry of Contrived Model No. 7: Furnace Slag No. 4 (2.83-6.35 mm) Topped with Particles of Itself $\leq 1\mu$ (Brightness (Arbitrary Units) versus Phase Angle..... 60

INTRODUCTION AND SUMMARY

This is the third of three interim reports on "Polarimetric Measurements of Simulated Lunar Surfaces," an investigation conducted under Contract No. NAS 9-4942. This report covers work done in Blue (0.48μ), Green (0.54μ), Visual (0.54μ), and Infrared (1.0μ) with contrived models during Phase III under the provisions of Proposal B.

As a result of Phase I conducted under this contract (Ref. 1), it was found that Volcanic Ash Nos. 1 and 4 and Coral No. 1 possessed average properties that could vary sufficiently in detail in integrated visual light to permit them to be considered as polarimetric models of the lunar surface. Two other materials (Furnace Slag No. 1 and Copper Oxide) could be considered as appropriate when combined with a suitable nonpolarizing material. Furnace Slag No. 4 and Silver Chloride were rejected because of a latitude dependence of polarization.

Phase II (Ref. 2) laid the basis for an analytical approach with an investigation of the polarization properties of materials as a function of particle size, albedo, and porosity. Current theories of polarization indicate that some of these properties are significant parameters.

Thus, as a result of Phase II, various samples were found to approximate the polarization extremes of lunar maria (Crisium) or highlands (Clavius). The best fit to Mare Crisium is obtained with Furnace Slag No. 4 particles less than 37 microns, Volcanic Ash No. 4 between 37 and 88 microns, Volcanic Ash No. 1 greater than 0.21 mm, the sponge-like slag obtained at NASA, and the Ash from Vesuvius. For Clavius, Furnace Slag No. 4 less than 1 micron, Volcanic Ash No. 4 between 1 and 37 microns, and Volcanic Ash No. 1 less than 1 micron are the best fits.

Phase III was undertaken so that the polarimetrically promising models of Phase I, which also were good photometrically by original selection, could be modified by sprinkling with the powders of Phase II to obtain a close match to lunar data in integrated and B, G, I light, as specified in Proposal B. Seventeen models were investigated on the Grumman large scale polarimeter and five required good models were obtained. An extra model, embodying the slag obtained at NASA/MSC, was modified to produce a good polarimetric model. Comparison to the lunar colorimetric curves of Gehrels (Ref. 5) reveals that Models 5 (Volcanic Ash No. 4 topped with particles of itself $\lesssim 1\mu$) and 6 (Volcanic Ash No. 1 topped with particles of itself $\lesssim 1\mu$) are the closest matches to Mare

Crisium with Model 6 being the overall best match. Model 1 (Slag, Sponge-like, topped with 0.088 to 0.21 mm particles of Volcanic Ash No. 1) is a fair match to Crisium. Models 2 (Coral No. 1 topped with Furnace Slag No. 4 particles $\leq$ 0.037 mm), 4 (Volcanic Ash No. 4 (chunks) topped with particles of Coral $\leq 1\mu$) and 7 (Furnace Slag No. 4 topped with particles of itself $\leq 1\mu$) are poor matches to the lunar surface with Model 2 coming closest to Clavius. The highest polarization occurs on all samples in the B(0.48μ) region where the albedo is lowest; the increase in albedo in the Infrared I(1.0μ) lowers the polarization similar to the lunar observations. The dependence of the location of the polarization maximum in relation to the maximum percent polarization cannot be determined from our data (Fig. 32). The inversion angle tends towards higher phase angles for decreased maximum polarization (Table 1). No clear trend is seen for the negative minimum percent polarization.

A check of the contrived models of Phase III has been made photometrically at a 60° viewing angle and Models 1, 6, 7, and 5 (Figs. 33, 37, 38, and 36, respectively) proved satisfactory in order of diminishing match; Models 4 and 2 (Figs. 35 and 34, respectively were unsatisfactory.

In essence, it has been shown in Phase III that a satisfactory photometric and polarimetric model may be constructed by combining a large scale photometric model that produces the shadowing necessary for good photometry (Ref. 3) with a powder that produces the scattering and refraction properties necessary for good polarization. The results are consistent with present knowledge of the lunar surface (Refs. 4 to 7). It remains to reconcile thermal, mechanical, and radar observations of the lunar surface. It appears possible that a high γ dust layer at the order of 1 mm thick ($\gamma = (K\rho c)^{-\frac{1}{2}}$ of the order of a few thousand) on top of the underlying material could explain some of the observed lunar thermal observations.

Percent polarization alone was observed in Phase II because the information obtained from plane of polarization observations in Phase II did not modify the results obtained from percent polarization.

The fundamental conclusion of Phase III is that the polarization properties of the lunar surface can be produced by a suitable particulate coating of the underlying material. This particulate coating could be the result of the deterioration of the underlying material into a dust by micrometeorite bombardment, and the resulting powder adhering to the lunar surface possibly by high vacuum bonding. Thus the surface properties could yield information on the underlying matter and ultimately give information as to the choice of good landing areas for the Apollo mission.

TEST EQUIPMENT

Description

The test equipment described in Phases I and II (Refs. 1 and 2) has been further improved under a Grumman supported program. The source in Phase II had produced a symmetrical beam with +1 percent residual polarization at the center. In addition, there was inadequate signal for good polarimetric observations at I (1.0μ) wavelength. The polarimeters had a residual polarization of +1/4 percent.

Source Polarization

The source was modified in a number of ways subsequent to the completion of Phase II. The clear 1000 watt source lamp was replaced with a frosted envelope lamp to reduce the lamp residual polarization. The source field stop was slightly off the optical axis, and by suitably realigning it, the source over-all residual polarization was reduced to 0.2 percent at the center with good symmetry around the periphery of the 3 inch diameter illuminated sample area.

Color filters, to permit B, G, and I photometry, previously had been mounted close to the 1000 watt source lamp. As a result, the filters were heated excessively, causing a change in their spectral response as well as frequent breakage. For polarization, large 6 1/2 inch square filters were obtained and mounted in a frame in front of the source lens housing closely perpendicular to the optical axis. The residual polarization of the filters was of the order of a tenth of a percent.

An increased capacity blower was installed on the source housing which permitted the lamp to be operated at rated value.

For the I (1.0μ) measurements, HR infrared polaroids were used since the usual HN-22 polaroids cease to be effective beyond 0.7μ.

Calibration

Percent Polarization - Calibrations of the polarimeter were made as described in Phase II for percent polarization, with

the exception that the lamp was operated at rated voltage of 120 V producing a system color response centered at 0.54μ as compared to 0.55μ for Phase II. The effective wavelength as quoted in Phase II (0.52μ) was incorrect due to the effect of an incorrect calibration on an additional filter inserted into the instrumental system. Albedo measurements were made as before with a system color response centered at 0.56μ because of the lower voltage (DOV) necessary on the source lamp in order not to saturate the photomultipliers.

The 6199 photomultipliers used for the B (0.48μ), G (0.54μ) and Visual (0.54μ) measurements were operated at 820 volts. The 7102 photomultipliers used for the I (1.0μ) measurements were operated at 1100 volts. The voltages were determined experimentally to produce the best average signal to noise ratios for the respective photomultiplier tubes.

A more detailed discussion of the technique mentioned will be reported in a forthcoming Grumman sponsored analysis of photometric and polarimetric procedures (Ref. 9).

STANDARD POLARIMETRIC CURVES AND DATA PRESENTATION

As in Phase II (Ref. 2) the analysis of data was made in terms of lunar observational information covering a range of values of percent polarization that served to differentiate lunar maria from highlands. As mentioned, the best detailed regional lunar polarization data appear to be that of Gehrels, Coffeen, and Owings (Ref. 5), the Russian observations appearing to be inaccurate.

Figures 1, 2, and 3 are plots of U (0.36μ), G (0.54μ), and I (0.94μ) data from Gehrels et al., for all lunar features observed. Since there were no B (0.44μ) data obtained by Gehrels et al., the U data may be compared with the B data in this report.

Referring to Fig. 1, the extreme polarization curves in U are those of Mare Imbrium and Clavius. For comparison purposes, the lowland curve for Mare Crisium is more complete than that of Mare Imbrium, since a maximum appears. Therefore, the Crisium curve was chosen as a comparison lowland curve to determine the relation of the experimentally observed maxima of Phase III to the lunar data. This reasoning applies similarly in Figs. 2 and 3 for G and I.

However, for the highland limiting curve, it appears that either Nicolai or Clavius would be appropriate. Since the Clavius curve is almost as complete as Nicolai, and appears to have less scatter for the Gehrels observed points, it was chosen. Incidentally, it can be seen that the location of the maximum on the Clavius curve moves to smaller angles as one goes from U to I or, synonomously, higher to lower polarization. This effect is not as clearly apparent for Crisium.

Thus, the limiting curves are those of Clavius and Mare Crisium for representative lunar highland and maria areas. In the curves to follow, a set of lunar comparison curves are presented on each of the Phase III experimental curves. For the section on Sample Preparation, the Gehrels limiting G curves are presented because they are closest to the Grumman polarimeter system in integrated visual light.

For subsequent Phase III experimental curves in B, G, and I light, the lunar G and I curves are presented for comparison

on each plot. The elimination of U as a graphical comparison was done because it does not correspond to the B observations of this report, and the graphs would be unnecessarily cluttered if it were included. For a comparison to the U, one can easily refer to the curve given in Fig. 1.

The albedos given are averages of those obtained in 1956/59 and 1963/64 by Gehrels et al. This is not strictly accurate because the lunar observational data on polarization have inherently an effect due to lunar luminescence, an effect that apparently varies with variations in solar activity (Ref. 5).

PHASE III – CONTRIVED MODELS

Purpose

Because certain of the models of Phase II duplicated the polarimetric properties of the lunar surface closely and others did not, an attempt was made to combine the photometrically and polarimetrically promising models of Phase I by sprinkling them with the appropriate powders from Phase II in order to closely duplicate the polarimetric properties of a representative lunar maria, a lunar highland, and intermediate areas. This procedure was followed in order to gain an insight into the physical properties and geometries of the lunar surface.

Test Specimens and Sample Preparation

The specimens chosen for investigation were those polarimetrically and photometrically promising from Phase I (Ref. 1), plus an additional specimen, the Furnace Slag obtained at NASA by one of the authors (W. G. Egan) in March 1965 (Ref. 2). The samples were chosen on the basis of observations made in integrated visual light with the 60° polarimeter. The 60° polarimeter was used in the model selection as it yields the most complete polarimetric curve from negative minimum and inversion, to positive maximum in one complete run. Comparison was made to the G (0.54μ) data of Gehrels et al., on Crisium and Clavius.

In order to prepare a sample, a choice was made for the base material, and then a second choice was made for the powder overcoat. Thus, for Contrived Model No. 1 (the extra sample), the Furnace Slag obtained at NASA was chosen. It can be seen graphically (Fig. 4) that the polarization of the Furnace Slag is too high; therefore a considerably lower maximum polarization material with a suitable inversion angle was chosen (0.088 to 0.21 mm particles of Volcanic Ash No. 1, having maximum polarization 8.4 percent at 93.5° phase angle and inversion at 24.5°, Ref. 2, p. 12, Table 1) and lightly dusted over the Furnace Slag to obtain a coating. The coating was dusted onto the furnace slag as an almost particulate cloud so that it settled lightly. Modifications of the over-all model were obtained by dusting more onto it or carefully dusting some off. The resulting composite curve closely matches that of Crisium (Fig. 4).

A similar procedure was followed for the remaining five required samples. A total of 17 variations of all samples was made before choosing the final versions.

The second sample, Contrived Model No. 2, was the original Coral No. 1 of Phase I (Ref. 1), lightly dusted with Furnace Slag No. 4 particles $\lesssim 0.037$ mm which had a maximum polarization of 14 percent at 111° phase angle, and an inversion at 18.5° (Ref. 2). After a few tries, the resulting curve of Fig. 5 was obtained, with a close match to Clavius.

The third sample, which was not used, was pieces of Volcanic Ash No. 4 on a 0.088 to .21 mm particulate Coral No. 1 background. The resulting curve was too poor to be considered.

The fourth sample was Volcanic Ash No. 4 (maximum polarization 17 percent at 113° phase angle Ref. 1). In order to reduce the maximum it was lightly dusted with coral particles $\lesssim 1\mu$ (maximum of >1.4 percent at $>125^{\circ}$ with an inversion at 27.5° Ref. 2). The coral was found to be a powerful depolarizer, and very little was required to produce the desired result shown in Fig. 6. The resulting polarization is intermediate between Clavius and Crisium being somewhat nearer to Clavius.

Contrived Model No. 5 consisted of large pieces of Volcanic Ash No. 4 (maximum polarization 17 percent at 113° phase angle, Ref. 1), which was dusted with $\lesssim 1\mu$ particles of itself. The attempt was to simulate a process that might occur on the lunar surface as a result of micrometeorite bombardment producing a thin fine dust layer. The $\lesssim 1\mu$ particles had a polarization maximum of 4.8 percent at 105° phase angle, and an inversion at 24° (Ref. 2). The result of the proper combination can be seen in Fig. 7 to be near to that of Crisium.

Contrived Model No. 6 uses the other volcanic ash, No. 1, with a dusting of $\lesssim 1\mu$ of itself. Volcanic Ash No. 1 has a maximum polarization of 20 percent at 115° (Ref. 1), whereas the $\lesssim 1\mu$ particles have a maximum of 5.8 percent at 99° phase angle, and an inversion at 25° (Ref. 2). The appropriate combination closely matches the polarization curve of Crisium (see Fig. 8).

With contrived Model No. 7, an attempt was made with the Furnace Slag No. 4 sample to produce a match to the lunar curves; the result was an intermediate curve shown in Fig. 9. Furnace Slag No. 4 has a maximum polarization of 39 percent at 130°

phase angle, while the $\leq 1\mu$ particles have a maximum of 9 percent at 115° and an inversion angle of 23° (Ref. 2). The combination produces an intermediate curve (Fig. 9).

Experiments

Percent Polarization

The percent polarization as a function of phase angle with color as a parameter for the five required and one additional sample is presented graphically in Figs. 11 through 27, and Table 1.

The data can be analyzed conveniently in terms of:

1. Wavelength and Phase Dependence of Percent Polarization
2. Effect of Color on Maximum Percent Polarization
3. Effect of Color on Normal Albedo
4. Effect of Color on Inversion Angle
5. Relationship between Normal Albedo and Maximum Percent Polarization
6. Relationship of Maximum Percent Polarization and the Corresponding Phase Angle
7. Incremental Color Changes on Percent Polarization as a Function of Sample

The correlation of the salient features on the percent polarization curves as a function of wavelength presented in Figs. 11 through 27 and Table 1 is shown graphically in Figs. 28 through 32. On all curves and in Table 1, a comparison is made to Crisium and Clavius as measured by Gehrels, et al. (Ref. 5).

Discussion of Results

Wavelength and Phase Dependence of Percent Polarization

Contrived Model No. 1 — Slag (sponge-like) topped with 0.088 to 0.21 mm particles of Volcanic Ash No. 1: Figures 10 (a) and 10 (b) are photographs of Contrived Model No. 1 taken

Table 1

DATA ANALYSIS

Sample	Albedo 0°	Albedo 60°	Percent Polarization Maximum %	Maximum Angle	Corrected Minimum %**	Corrected Minimum Angle	Corrected Inversion Angle**
No. 1 Slag (Sponge-like) topped with 0.088 to 0.21 mm particles of Volcanic Ash No. 1							
B (0. 48μ)	.12	.09	13.2	99°	-1.8	12°	25.0°
Visual (0.54μ)	.17	.13	11.5	114	-1.4	12	25.5
G (0.54μ)	.14	.09	10.7	106	-1.7	11	24.5
I (1.0μ)	.31	.28	4.6	100	- .9	10	25.5
No. 2 Coral No. 1 topped with Furnace Slag No. 4 particles ≤ 0.037 mm							
B	.11	.17	5.4	85	<-1.0	<-3.5	19.5
Visual	.12	.18	5.8	81	<-1.2	<-2.5	17.5
G	.14	.18	5.2	82	- .8	5	18.5
I	.13	.19	3.5	77	- .8	7.5	22.0
No. 4 Volcanic Ash No. 4 (Chunks) topped with particles of Coral ≤ 1μ							
B	.17	.19	10.2	118	-1.4	8	22.0
Visual	.19	.21	10.6	121	-1.2	9.5	22.5
G	.18	.20	9.9	123	<-1.2	<3	23.0
I	.27	.30	6.9	118	-1.0	6	25.5
No. 5 Volcanic Ash No. 4 topped with particles of itself ≤ 1μ							
B	.13	.18	13.9	95	-1.7	9	23.0
Visual	.16	.14	10.1	94	-1.4	9	23.0
G	.15	.13	12.1	94	-1.6	8.5	22.5
I	.27	.27	6.3	97	- .9	8	24.5
No. 6 Volcanic Ash No. 1 topped with particles of itself ≤ 1μ							
B	.11	.10	18.0	99	-2.1	9.5	24
Visual	.14	.14	13.2	99	-1.9	9	24
G	.12	.12	15.0	103	-1.9	10	23.5
I	.25	.25	8.0	105	<-1.0	<3	26.5
No. 7 Furnace Slag No. 4 topped with particles of itself ≤ 1μ							
B	.12	.10	12.9	121	-1.1	9.5	22.5
Visual	.12	.12	10.3	118	- .9	8.5	23.5
G	.13	.11	12.8	119	-1.1	11	24
I	.12	.12	10.2	117	- .9	11	27
Crisium U (0.36μ)	.087		22.0	100	-1.2	10	20.7
G (0.54μ)	.137*		12.5	102	-1.2	11	23.7
I (0.94μ)	.206		8.3	98	-1.2	12.5	24.3
Clavius U (0.36μ)	.175		~9.5	>98	-1.0	10	22.1
G (0.54μ)	.268*		5.8	91	-0.9	11	25.0
I (0.94μ)	.401		4.4	82	-1.1	8	22.2

*Average albedos determined in V (0.55μ) from Gehrels et al.

**Minimum Percent Polarization and Inversion Angle are corrected for +1/4 percent Residual Polarization of Polarimeters

at 0° and 65° illumination angles at 10° viewing angle with the same exposure to show shadowing effects. In order that the camera not block the incident illumination, it was displaced out of the plane of incidence by 10° to the average normal of the sample. The Furnace Slag was obtained, as mentioned previously, by one of the authors (W. G. Egan) from the astronaut training pit at NASA/MSC. The sample was selected in March 1965 as representative of the lunar surface, as well as could be determined, from a visual inspection. The necessary shadowing features for good photometry were evident, and it appeared dark enough in order to produce sufficient polarization. As modified with 0.088 to 0.21 mm particles of Volcanic Ash No. 1 used in this program, it generally matches Mare Crisium (Fig. 11 and Table 1). The integrated visual light curve V (0.54μ) shown (used for matching, see Fig. 4) is within about 1 percent of the Crisium standard G (0.54μ) curve at the upper portion, and much closer at the lower portion; however, the upper portion of the contrived model curve deviates from the general trend of Crisium. The use of the Gehrels et al. G curve to compare to the contrived model measured in integrated visual light (0.54μ) appears legitimate in terms of the effective wavelengths; however, this does not take into account for the shape of the response of the system as it washes out in the determination of the effective wavelength. Thus, it is seen that the contrived model G curve (0.54μ) closely follows the curve shape of the standard G (0.54μ) curve at larger phase angles, since perhaps the effect of the red end of the spectrum is minimized. The contrived model can be seen to produce a decrease in polarization of 6.1 percent between G and I, and hence the contribution of the I to the Visual response can be significant. At phase angles below inversion the polarization produced by the contrived model in I (1.0μ) is greater than the standard I (0.94μ), with a higher corrected inversion angle (see Table 1). Also, at angles above inversion, the observed polarization is less than that for the lunar standard. A portion of this effect is possibly the result of the I measurements for Phase III being made at 1.0μ as contrasted to the standard at 0.94μ.

The trend of higher maximum polarization with lower albedo found in Phase II (Ref. 2) is followed in Phase III where the albedo changes as a function of color instead of as a function of particle size as in Phase II. However, there are variations between the 0° and 60° albedos. The 0° albedos are consistently higher than the 60° albedos, and this is attributed to the method of deposition of the Volcanic Ash and the configuration of the Furnace Slag. The Volcanic Ash No. 1 did

not adhere as well to the vertical surfaces of the Furnace Slag as it did to the horizontal surfaces. Since the albedo of the Volcanic Ash No. 1 in the size range 0.088 to 0.21 mm is 0.15, compared to 0.11 for the sponge-like Slag (see Table 1, p. 12, Ref. 2), the volcanic ash increased the 0° albedo above the 60° albedo. Referring to Fig. 12, where the effect of polarimeter viewing angle is presented, it can be seen that, above the inversion angle, the 60° polarimeter measures a higher polarization than the 0° polarimeter which is consistent with the lower albedo at 60° viewing angle. The effect on the minimum and inversion angle is more complicated. However, photometrically, we have an unusual sample with a composite albedo. This will be elaborated upon subsequently in the section on Lunar Implications.

Contrived Model No. 2 — Coral No. 1 topped with Furnace Slag No. 4 particles $\leq$ 0.037 mm: Figures 13 (a) and 13 (b) are photographs of Contrived Model No. 2 taken at 0° and 65° illumination angles to show again the effect of shadowing. The coral was also subject to the limitations mentioned for Contrived Model No. 1 in that the particles of Furnace Slag No. 4 dusted upon it adhered to the areas where the coral was rough. Certain vertical areas where the coral was broken did not pick up much furnace slag, and, in general, vertical surfaces picked up less than horizontal surfaces.

The curves shown in Fig. 14 indicate a match (within 1.5 percent) to Clavius which is fair at phase angles below the maximum (compare Visual 0.54μ with Clavius G 0.54μ), but very poor above the maximum. The general shapes of the B, G and I curves for the sample are similar, with a displacement of the maximum toward higher polarizations from I through G to B. The Visual curve is higher than either the B, G, or I curve, contrary to the effect on Contrived Model No. 1 where the Visual is lower than the B above the inversion angle (Fig. 11). Thus, it appears that the combination of percent polarizations is not a simple additive one for color.

The trend toward higher maximum percent polarization for decreased albedo can be discerned above the experimental error (see Table 1). The effect of non-uniform distribution of the Furnace Slag No. 4 particles on the Coral No. 1 can be seen in the consistently higher albedos for the viewing angle of 60° (see Table 1). The vertical surfaces are whiter, producing a higher albedo at 60°. However, an exception occurs in that

the higher albedo does not clearly produce a lower polarization at higher phase angles, (see Fig. 15). Because of the complicated shadowing nature of the coral, the trend of lower polarization for higher albedo is not followed.

Contrived Model No. 4 — Volcanic Ash No. 4 (chunks) topped with particles of Coral $\lesssim 1\mu$: This sample is shown in Figures 16 (a) and (b). The effect of the white coral on the increase in albedo is readily apparent.

The polarimetric results can be seen in Fig. 17, and are intermediate between Clavius and Crisium, but nearer the former, to which it is compared. The general curve shape is good except that the maximum occurs at too large an angle to be comparable to the lunar surface. The high maximum polarization of Volcanic Ash No. 4 of 17 percent at 113° phase angle (see Ref. 1, p. 17, Table 9), has been altered by the coral in effect reducing the maximum to 10.6 percent and increasing the location of the maximum to 121° in Visual light. The peculiar effect of the coral in giving in a Visual percent polarization above the B, G, and I curves was also noted for Contrived Model No. 2. There is not much difference between the maximum percent polarization in the B, G, or Visual curves for Model No. 4; also the differences are small in regard to the negative minimum for B and G. The higher minimum value for the I may possibly be the cause of the increase in the V minimum (see Fig. 17). For phase angles between 26 and 67 degrees, the contrived model in I lies fairly close to the standard I curve for Clavius, but it differs greatly above 67°.

The trend of higher maximum polarization for lower albedo is followed, with the slight trend to higher albedos for the 60° viewing angle. This small difference in albedo is the result of the mode of sample preparation where the vertical surfaces pick up more coral than the horizontal surfaces, resulting in a slightly higher albedo at 60° viewing angle. Referring to Fig. 18, it can be seen that usual albedo-polarization trend is observed, the higher albedo produces lower polarization at large phase angles. This shows that the coral is dominated by the effect of the base material.

Contrived Model No. 5 — Volcanic Ash No. 4 (chunks) topped with particles of itself $\lesssim 1\mu$: This sample is shown in Fig. 19 (a) and (b) at 0° and 65° illumination angles. It is to

be remarked that all photographs have been taken at the same exposure in order to permit a relative appraisal of the photometric properties from the photographs.

The polarimetric curves shown in Fig. 20, and summarized in Table 1, reveal a trend following closely the lunar data for Crisium. Contrary to the curves involving coral (either coral on a base material [Model No. 4] or another material on coral [Model No. 2]), the Visual curve lies below the G curve, as expected, possibly being the result of the lower polarization contribution of the red end of the system response. The B and G curves following closely the shape of the standard differ mainly in the magnitude of the maximum, B being at 13.9 percent and G at 12.1 percent, which is to be expected as the albedos are 0.13 and 0.15 respectively. The corrected inversion angles are low by about 1°. The minimum percent polarization for I is greater than Crisium by 0.3 percent. (The B and G negative polarizations are slightly low).

The albedos at 0° and 60° do not show any clear trend resulting from sample preparation. Possibly the Visual zero degree albedo is higher because the $\lesssim 1\mu$ powder has an albedo of 0.195 (Ref. 2, p. 12, Table 1) and the chunks have an albedo of 0.14 (Ref. 1, p. 17, Table 9), with the effect previously noted that the horizontal surfaces predominately viewed at 0° would have the higher albedo. An exception occurs for the B albedo measurement where the 60° reading is higher, possibly the result of a surface color of the underlying chunks of Volcanic Ash.

The highest albedo (0.27) occurs at I, and this curve has the lowest maximum percent polarization, even lower than Crisium (albedo 0.206). It is probable that, as remarked before, the observations of I in Phase III at 1.0μ, compared to the lunar standard observation at 0.94μ, would produce a lower polarization because of the higher albedos toward the infrared (Ref. 10).

Overall, this sample is a fair match to Mare Crisium.

There appears to be an effect due to viewing angle (Fig. 21), the 60° curves being higher than the 0° curves. This is most probably the effect of the higher maximum polarization of the base material (17 percent; Ref. 1, p. 17, Table 9) as

compared to the topping material (4.8 percent; Ref. 2, p. 12, Table 1). The base material would be seen more at the higher viewing angle because the powder would not adhere to the vertical surfaces.

Contrived Model No. 6 — Volcanic Ash No. 1 (chunks) topped with particles of itself $\lesssim 1\mu$: Photographs of this sample are shown in Figures 22 (a) and (b). This sample appears to be the best lunar model, on the basis of these photographs alone, Fig. 22 (b) bearing a close resemblance to the photographs obtained by the Luna 9 vehicle (Ref. 4).

Referring to Fig. 23, it is seen that the curves for B, G and I are close matches of the shapes obtained from lunar observations. It is rather significant that the I curve obtained is slightly higher than the lunar I curve in the region of negative polarization below the inversion angle. Even though a good match in the visual region is obtained, this does not mean that a good match would be observed in the infrared. Since our observations are slightly redder than Gehrels et al., the observed effect could be indicative of what is to be expected when the selected terrestrial samples are examined in longer wavelength infrared. Additional evidence is obtained by referring back to Contrived Model No. 5; the same diminished polarization minimum is observed. This phenomena is elaborated upon in the subsequent section on Conclusions.

The general overall curve trend is excellent, with the maximum percent polarization for the B being above the G, and G being above the Visual. The I curve is the lowest, and the trend is borne out by the relationship between the respective albedos. The Visual curve lies below the G curve since it has a higher albedo resulting from the higher albedo toward the red. The volcanic ash has a brownish appearance, indicating material with a higher reflectivity in the red.

There is a slight effect of viewing angle (Fig. 24) also most probably the result of the higher maximum percent polarization base material (20 percent; Ref. 1, p. 17, Table 9) compared with the topping powder (5.8 percent; Ref. 2, p. 12, Table 1). The effect is small indicating a fairly good distribution of the $\lesssim 1\mu$ powder on the base material.

Overall, this is the sample which gives the best match to the lunar surface based on polarization-wavelength measurements, remembering the infrared anomaly mentioned.

Contrived Model No. 7 — Furnace Slag No. 4 (2.83 to 6.35 mm) topped with $\lesssim 1\mu$ of itself: This sample is shown in Figures 25 (a) and (b).

The polarimetric results are depicted in Figure 26. The model lies between Clavius and Crisium being relatively closer to Crisium. It is unusual that the polarization in G is considerably larger than in Visual light. It is not a very good match, since the maxima for B, G, I, and Visual occur at around 120° compared to about 100° for Crisium. There is a peculiarity in that the peak of the Visual curve lies very close to the I curve. As the albedos are the same, within experimental error, for B, G, and I, the substance appears gray.

The minima are greater than the -1.2 percent required for a match to Crisium, and the I inversion angle is too high by about $2\ 1/2^{\circ}$.

The viewing angle dependence, shown in Fig. 27, indicates that the polarization is higher for a zero degree viewing angle, above a phase angle of about 43°. This may possibly be attributed, as previously, to the viewing of the base material at the 60° viewing angle because as the base material has a higher maximum polarization (41 percent; Ref. 1, p. 17, Table 9) than the topping powder (9 percent; Ref. 2, p. 12, Table 1).

Effect of Color on Maximum Percent Polarization

In Fig. 28, a comparison of maximum percent polarization as a function of reciprocal wavelength in $(\text{microns})^{-1}$ is presented, together with comparison curves from Gehrels et al., for Crisium and Clavius. For a perfect match, the curve for the contrived model should lie upon one of the lunar curves. Thus, Contrived Model No. 5 (Volcanic Ash No. 4 topped with $\lesssim 1\mu$ particles of itself) is seen to be a good fit with No. 6 (Volcanic Ash No. 1 topped with $\lesssim 1\mu$ particles of itself) being the next best fit. Contrived Model No. 2 (Coral No. 1 topped with Furnace Slag No. 4 particles $\lesssim 0.037$ mm) appears to be a good fit to Clavius, based on this criterion alone. Contrived Models No. 1 (Slag topped with 0.088 to 0.21 mm particles of Volcanic Ash No. 1), No. 4 (Volcanic Ash No. 4 topped with particles of Coral $\lesssim 1\mu$) and No. 7 (Furnace Slag No. 4 topped with particles of itself $\lesssim 1\mu$) are poor fits to the lunar data.

It must be remembered that the maximum polarization wavelength dependence is only one of the criteria for lunar comparison. What is involved here is the relative maximum polarization, and this is only one feature of the entire polarization — phase angle curve.

Effect of Color on Albedo

The effect of color on the observed normal albedo is plotted in Fig. 29. It is seen that Contrived Models Nos. 5 and 6 are fair matches to Crisium, as they were in terms of maximum polarization mentioned in the previous section. Contrived Models No. 2 and 7 are poor matches, even though Model No. 2 was a good match in terms of maximum polarization. Model No. 1 is a questionable match, having a higher curve slope than Crisium. Model No. 4 is parallel to Crisium and therefore a good color fit.

The physical property involved here is color of the sample. If the sample is reddish or brownish, it would have a higher albedo in the red, as does the lunar surface.

Effect of Color on Inversion Angle

It is seen in Fig. 30 that for the six samples a comparison of the effect of color on the inversion angle shows an increase in the inversion angle as the wavelength increases from G to I ($1/\lambda$ decreasing from 1.85 to $1.0\mu^{-1}$). No such trend can be discerned between B and G ($1/\lambda$ decreasing from 2.08 to $1.85\mu^{-1}$). Clavius shows an opposite trend between G and I with decreasing inversion angle with increasing wavelength. However, the inversion angle increases with increasing wavelength between U and G. For Crisium the inversion angle remains fairly constant with increasing wavelength between G and I, while it increases between U and G.

None of the contrived model curves from Phase III have the same inversion angle-color dependence as the lunar standards. Therefore this criterion cannot be used effectively to differentiate between adequate simulated lunar surface models.

Essentially, the inversion angle appears to be an effect tied up in the overall details of surface polarization.

Relationship between Albedo and Maximum Percent Polarization

In Fig. 31 is plotted a comparison of the maximum polarization and normal albedo for the six samples together with the standard curves of Clavius and Crisium. It is seen that Contrived Models No. 2 and 7 (the Coral No. 1 topped with Furnace Slag No. 4 and Furnace Slag No. 4 topped with itself) are not appropriate matches to the lunar surface. Samples 1, 4, 5 and 6 have approximately the same slope as Clavius and Crisium while differing slightly in their zero points.

An empirical relationship has been mentioned between polarization and normal albedo by Clarke (Ref. 11), and the general trend of decreasing albedo with increasing maximum percent polarization is observed for all models which we consider to be good matches.

Relationship of Maximum Percent Polarization and the Corresponding Phase Angle

Figure 32 depicts the relationship between maximum percent polarization and the corresponding phase angle for the six Contrived Models and the lunar standards. Models No. 1, 2, 4 and 7 as well as Clavius seem to show a decrease of the position of the maximum polarization as the maximum value decreases. Models No. 5 and 6 seem to show the opposite effect while Crisium apparently shows no dependence.

It is not yet clear if the phase angle of maximum polarization is a basic parameter of the polarization curve. Possibly some additional experiments could clarify this effect.

Incremental Color Changes of Percent Polarization as a Function of Sample

A rough evaluation of the amount of polarization change for each sample as a function of color change yielded no significant results. The increment in polarization going from I to G depended upon the sample, as well as the increment going from G to B. This sample dependence on incremental color changes should be extended to allow one to determine the characteristics of a possible lunar landing area using polarization techniques.

Lunar Implications

Thus far, the emphasis has been on the polarimetric properties of the contrived models investigated. Although not required for the contract, photometric observations were made, under a Grumman supported program, in order to augment the integrated multi-disciplined approach to the definition of the lunar surface. These curves are presented in Figs. 33 through 38. A good photometric match is obtained from Contrived Model No 1, the Furnace Slag (from NASA) topped with 0.088 to 0.21 mm particles of Volcanic Ash No. 1 (see Fig. 33 [a] and [b]). A 60° viewing angle photometric run was made in order to observe not only the low phase angle opposition effect, but to observe the effect of the sample at high phase angles. Because the normal albedo was lower as a result of the composite albedo effect, a zero degree viewing angle curve was run (Fig. 33 b). The match is good on one side, but not on the other because of non-uniformities in the sample.

An equally good match was Contrived Model No. 6 (Fig. 37) which was the best polarimetric match. In descending order of match are Contrived Models 7 and 5 (Figs. 38 and 36), but the deviations are small.

The samples utilizing coral in any form (Contrived Models No. 4 and 2) were unsatisfactory photometrically (see Figs. 35 and 34). As a check on Contrived Model No. 2, (Coral No. 1 topped with Furnace Slag No. 4 particles), a zero degree photometric curve was run. It is seen that the zero degree viewing angle photometer produces a poor match (Fig. 34 b). The normal albedo for Contrived Model No. 2 was found to be lower because of the non-adherence of the slag to the vertical surfaces. This produced a darker sample when viewed in the normal direction relative to being viewed at 60°, thus constituting a composite albedo.

It is of interest to consider the opposition effect, relative to the normalization at 4°. A good opposition effect at 60° viewing angle is observed for Contrived Models No. 1, 6, 7, 5, 4, 2 in order of which is the same order of decreasing photometric match.

The following criteria were used to evaluate the relative merits of the six contrived models:

(1) Percent Polarization Curves Integrated Visual Light

(2) Percent Polarization Curves, B, G, and I Light

(3) Albedo-Color Relationship (Fig. 29)

(4) Albedos at Zero and 60° Viewing Angles

(5) Albedo-Maximum Percent Polarization (Fig. 31)

(6) Maximum-Percent Polarization — Color Relationship (Fig. 28)

(7) Photometry

(8) Uniformity of Polarization — Zero and 60° Polarimeter

Thus, using the lunar data of Gehrels et al., Models 5 and 6 are the closest matches to Mare Crisium, with Model 6 being the overall best match. Model 1 is a fair match to Crisium. Models 2, 4, and 7 are poor matches with Model 2 coming closest to Clavius.

It has been observed that the highest polarization occurs on all samples in the B (0.48μ) where the albedo is the lowest; the increased albedo in the infrared I (1.0μ) lowers the polarization, similar to the lunar observations. The dependence of the location of the polarization maximum in relation to the maximum percent polarization cannot be determined from our data (see Fig. 32). The inversion angle tends to higher phase angles for decreased maximum polarization. No clear trend is seen for the negative minimum percent polarization (see Table 1).

CONCLUSIONS

In essence, it has been shown in Phase III that a satisfactory photometric and polarimetric model may be constructed by using a large scale photometric model that produces the shadowing necessary for good photometry (Ref. 3) with a powder that produces the scattering and refraction properties necessary for good polarization (Ref. 2). The results obtained here are consistent with present knowledge of the lunar surface (Refs. 4 to 7).

The results obtained remain to be reconciled with thermal, mechanical and radar observations of the lunar surface. It appears possible that a thin dust layer of the order of 1 mm thick ($\gamma = (K\rho c)^{-\frac{1}{2}}$ [Ref. 8] of the order of a few thousand) on top of the underlying material could explain some of the observed lunar thermal observations (Ref. 8 and J. Reichman — private communication).

The fundamental conclusion of Phase III is that the polarization properties of the lunar surface can be produced by a suitable particulate coating of the underlying material. This particulate coating could be the result of the deterioration of the underlying material into a dust by micrometeorite bombardment, and the resulting powder adhering to the lunar surface possibly by high vacuum bonding. Thus the surface properties could yield information on the underlying matter and ultimately give information as to the choice of good landing areas for the Apollo mission.

RECOMMENDATIONS

As a result of the work carried out in Phase III, as well as that pursued previously, additional recommendations that would appear fruitful are:

1. Additional investigations of material properties are required in order to define the engineering properties of materials that yield the proper lunar polarimetric and photometric signatures. Typical investigations might be differential thermal analysis and X-ray diffraction.

2. Extension of infrared investigations to 1 to 3μ and 8 to 14μ for simulated lunar samples in terms of the over-all integrated interdisciplinary approach (see Ref. 10 as an example).

3. Investigation of luminescence as it affects albedo and polarization in an effort to elucidate the material composition of the lunar surface.

4. Investigation of incremental color changes as an index of lunar landing area characteristics.

5. Investigation of the effect of simulated solar wind effects on the best contrived models.

REFERENCES

1. Egan, W. G. and Smith L. L., Polarimetric Measurements of Simulated Lunar Surfaces, Grumman Research Department Memorandum RM-304, First Progress Report on NASA Contract No. NAS 9-4942, December 1965.

2. Egan, W. G. and Smith, L. L., Polarimetric Measurements of Simulated Lunar Surfaces, Phase II, Grumman Research Department Memorandum RM-312, Second Progress Report on NASA Contract No. NAS 9-4942, February 1966.

3. Halajian, J. D. and Spagnolo, F. A., Photometric Measurements of Simulated Lunar Surfaces, Quarterly Progress Report, Contract No. NAS 9-3182, Grumman Research Department Memorandum RM-308, January 1966.

4. New York Times, February 6, 1966, "Moscow Releases Two of Its Moon Photos," p. 1.

5. Gehrels, T., Coffeen, T., and Owings, D., "Wavelength Dependence of Polarization. III. The Lunar Surface," Astronomical Journal, 69, No. 10, December 1964, pp. 826-852.

6. Halajian, J. D., Photometric Measurements of Simulated Lunar Surfaces, Second Interim Report on NASA Contract No. NAS 9-3182, Grumman Research Department Memorandum RM-262, January 1965.

7. Egan, W. G., Polarimetry and the Lunar Surface — A Literature Survey, Grumman Research Department Memorandum RM-271, April 1965.

8. Halajian, J. D. and Reichman, J., Correlation of Mechanical and Thermal Properties of Extraterrestrial Materials, Second Quarterly Progress Report on Contract NAS 8-20084, Grumman Research Department Memorandum RM-309, February 1966.

9. Egan, W., et al., Search for a Lunar Surface Model — Appendix A: Analysis of Photometric and Polarimetric Equipment, Grumman Research Memorandum (in preparation).

10. Binder, A. B., Cruikshank, D. P., and Hartmann, W. K., Observations of the Moon and of the Terrestrial Rocks in the Infrared, Icarus 4, p. 415-420 (1965).

11. Clarke, D., The Wavelength Dependence of the Polarization of Light Reflected by the Moon and Mars, Monthly Notices Royal Astr. Soc., Vol. 130, No. 1, p. 83, 1965.

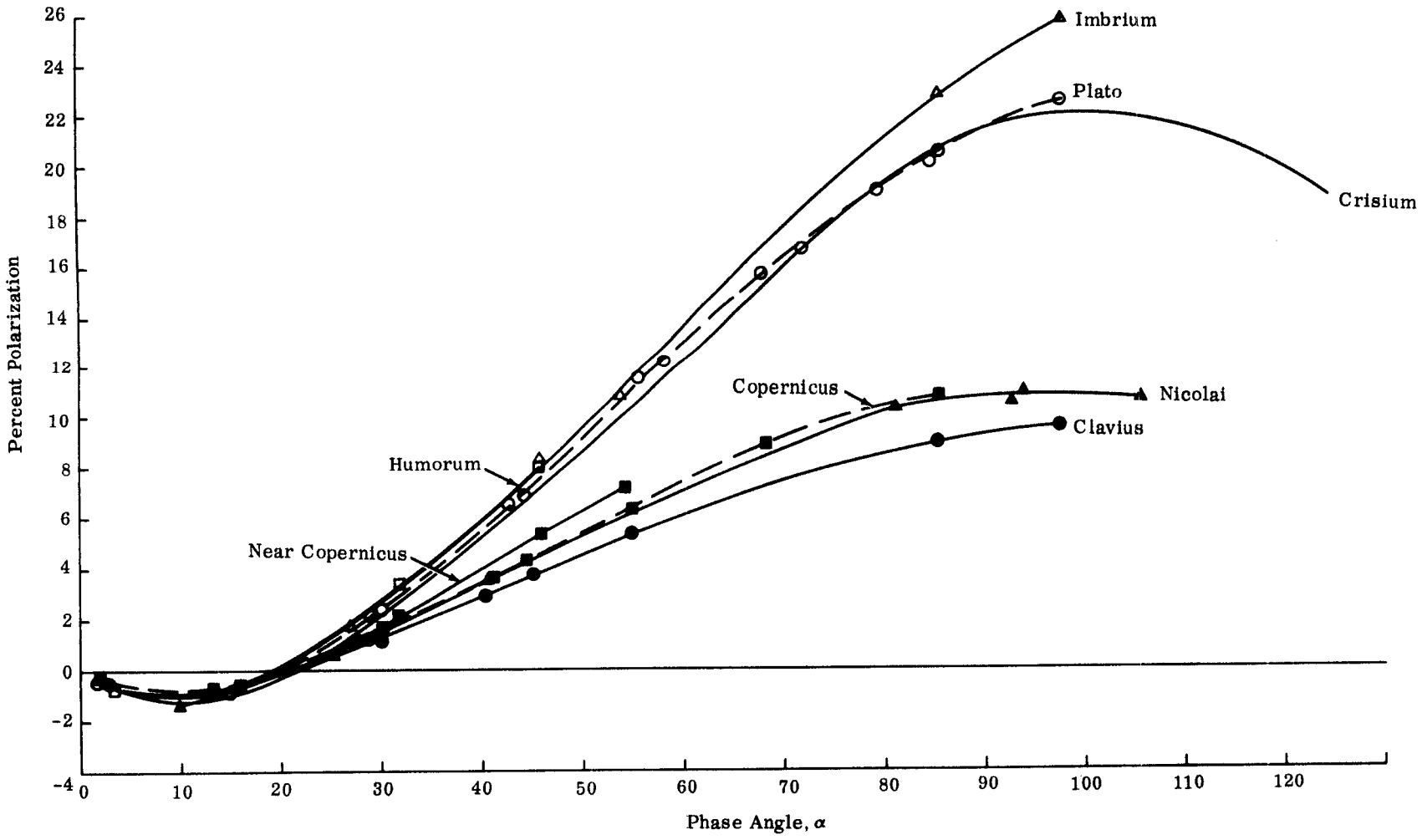

Fig. 1 Polarization Curves of the Moon -- Ultraviolet Range, 0.36μ (Gehrels et al.)

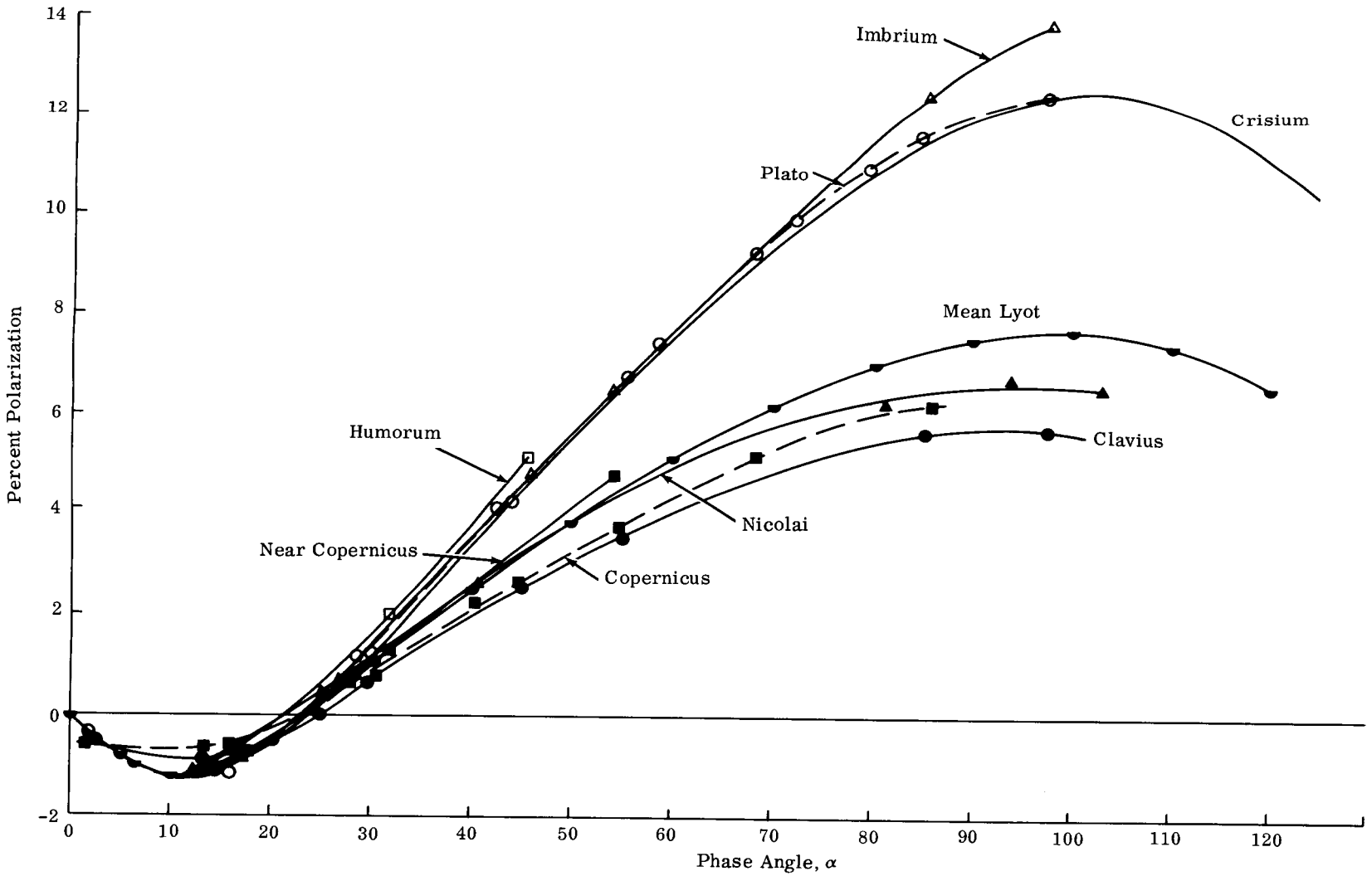

Fig. 2 Polarization Curves of the Moon -- Green Range, 0.54μ (Gehrels et al.)

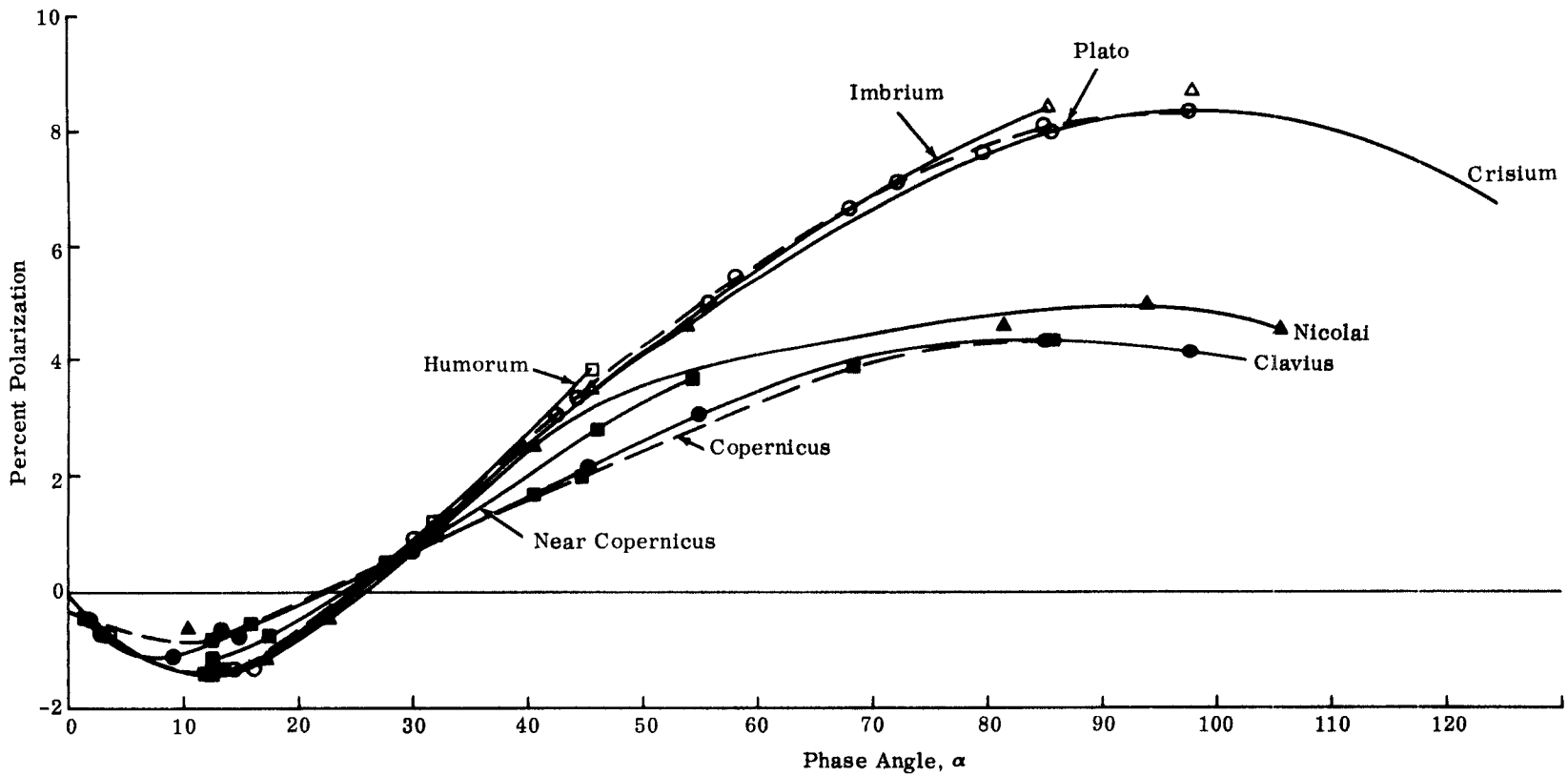

Fig. 3 Polarization Curves of the Moon -- Infrared Range, 0.94μ (Gehrels et al.)

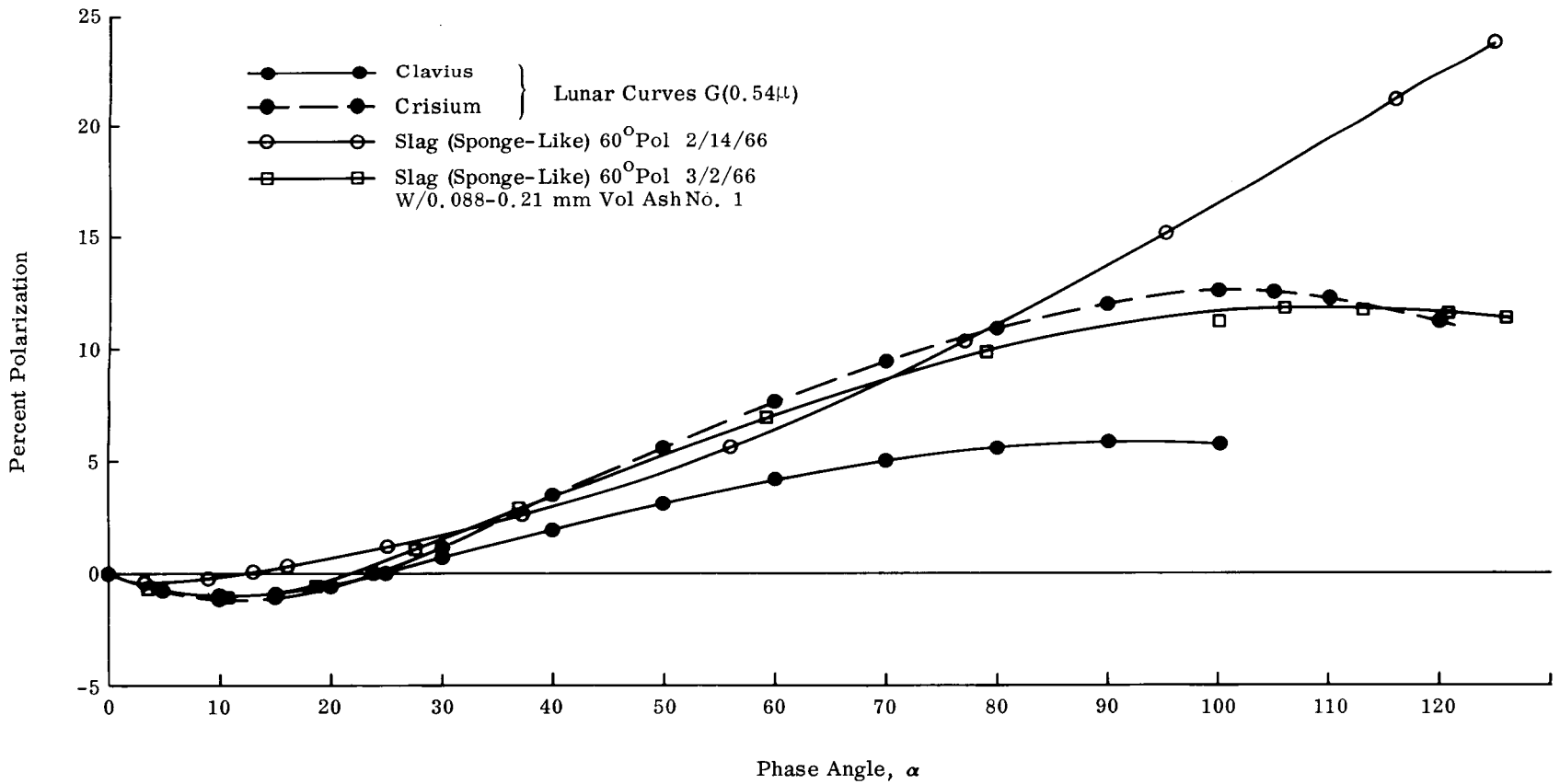

Fig. 4 Contrived Model No. 1 Development

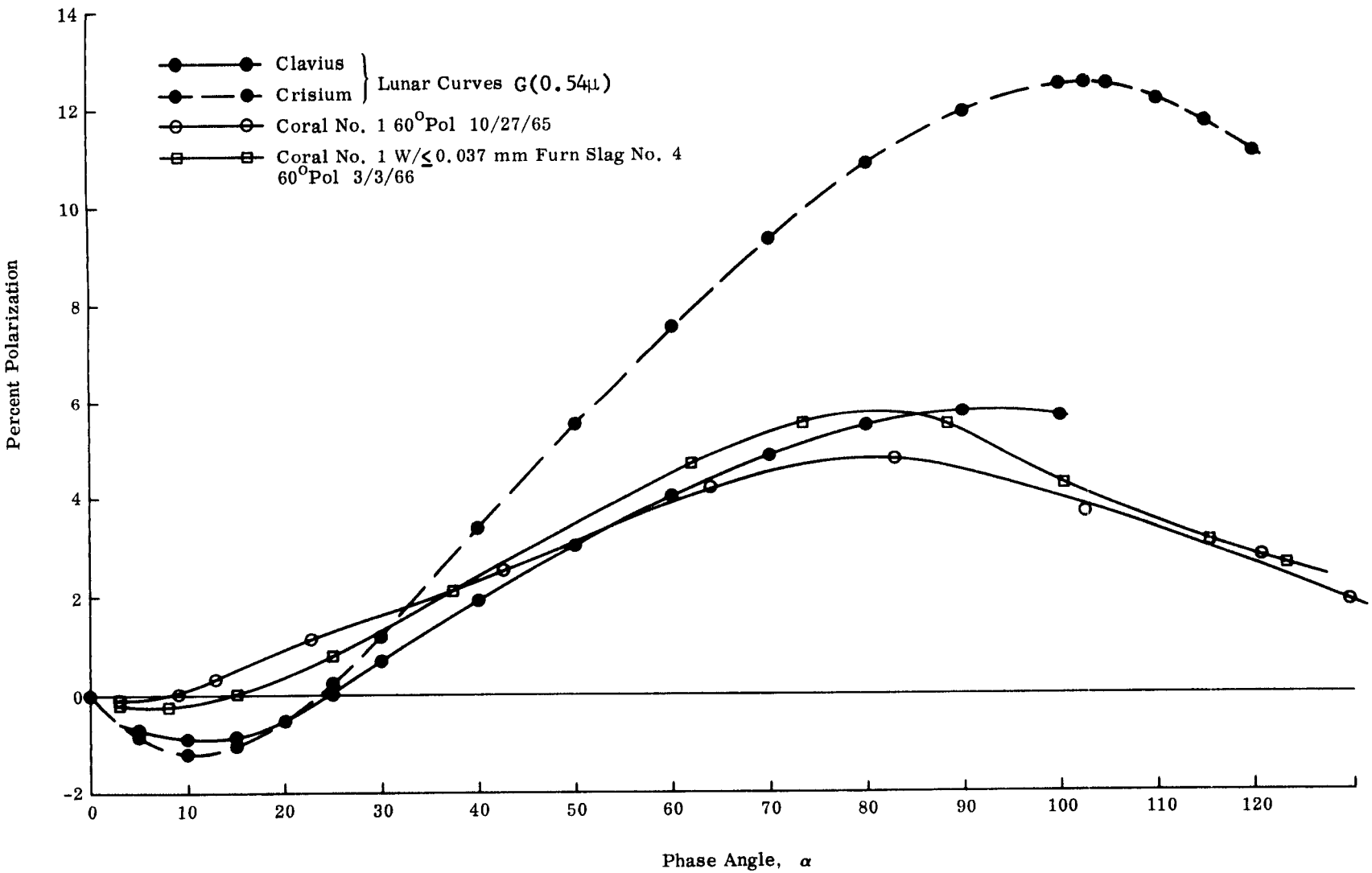

Fig. 5 Contrived Model No. 2 Development

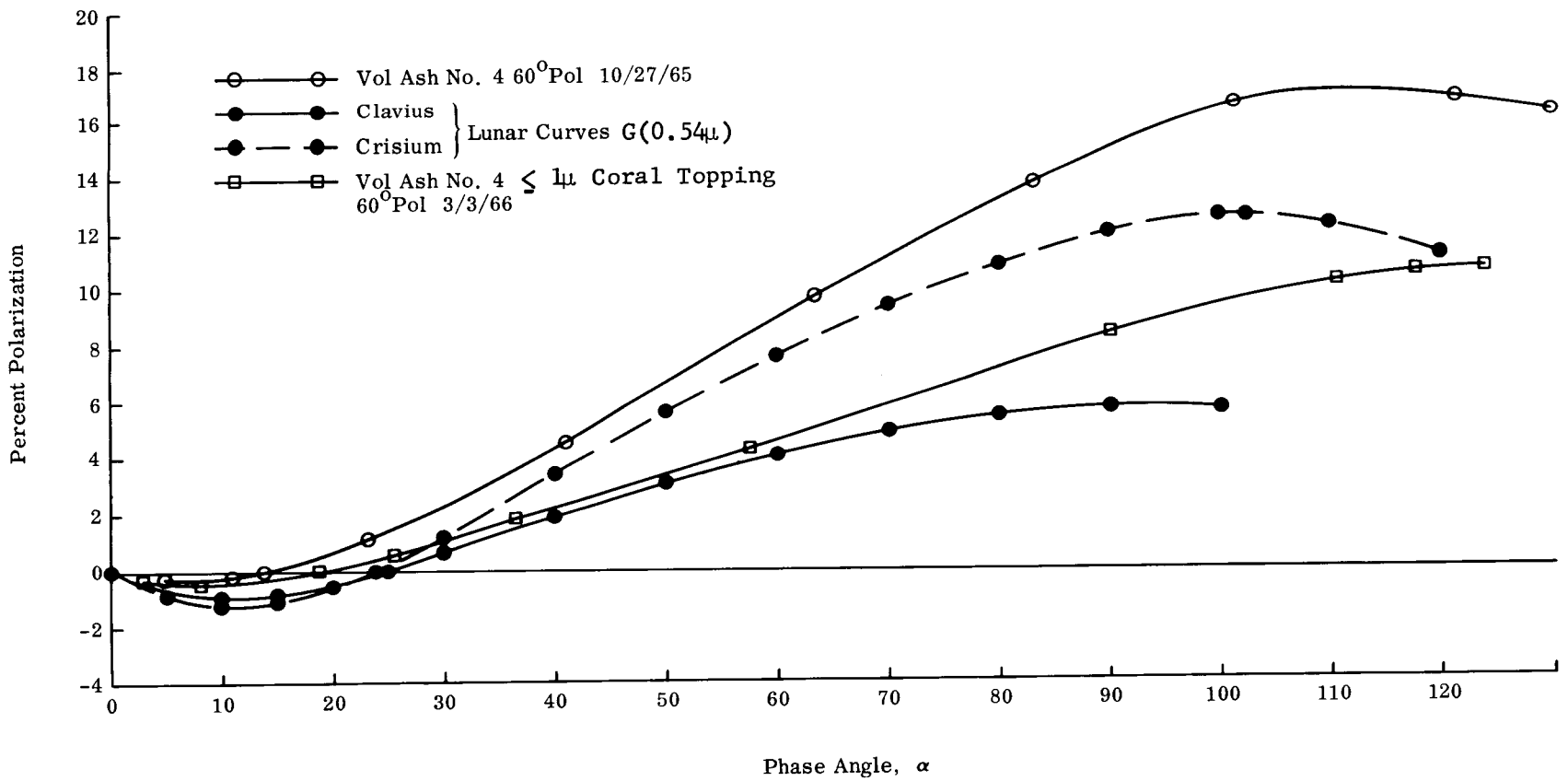

Fig. 6 Contrived Model No. 4 Development

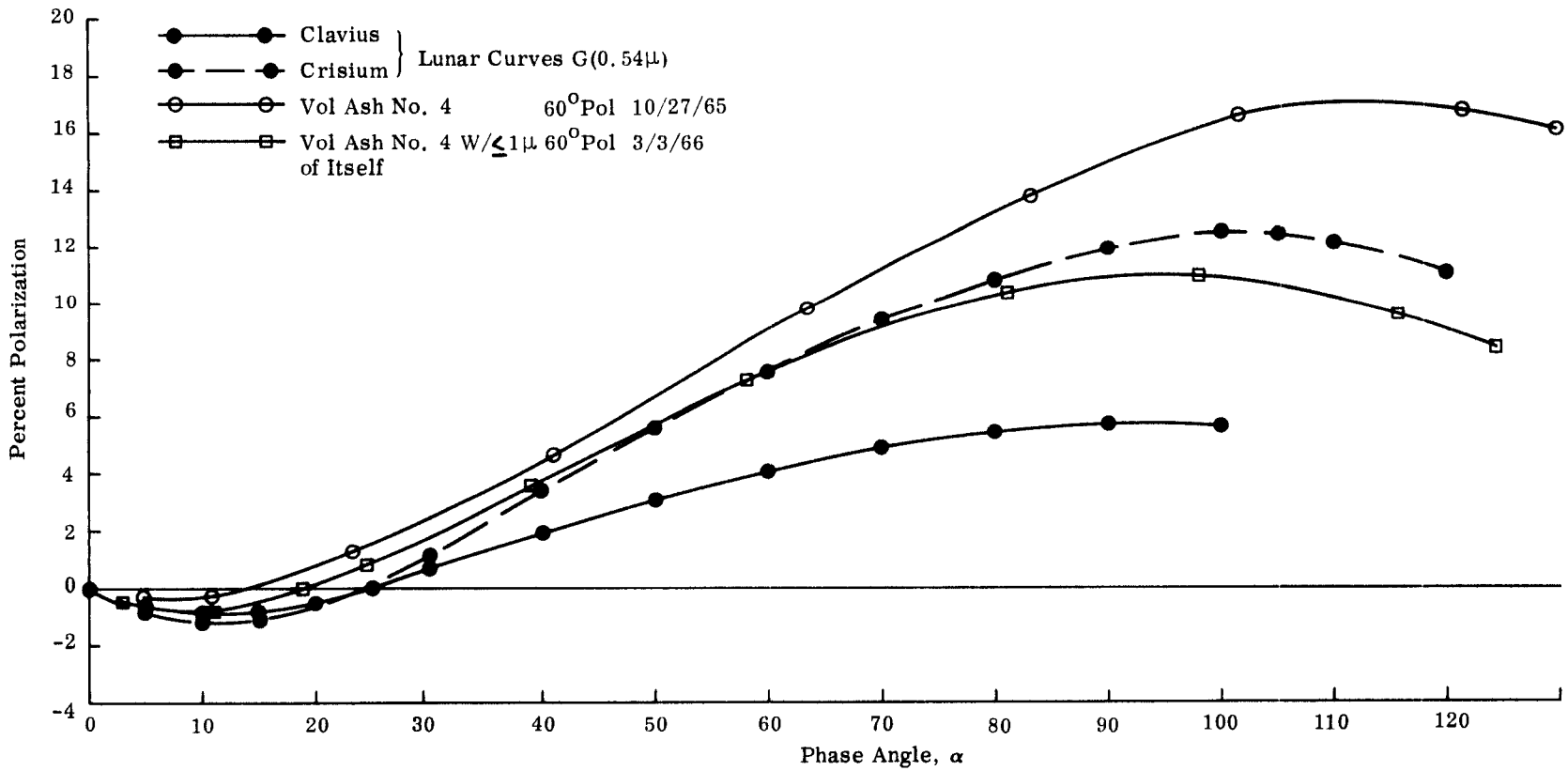

Fig. 7 Contrived Model No. 5 Development

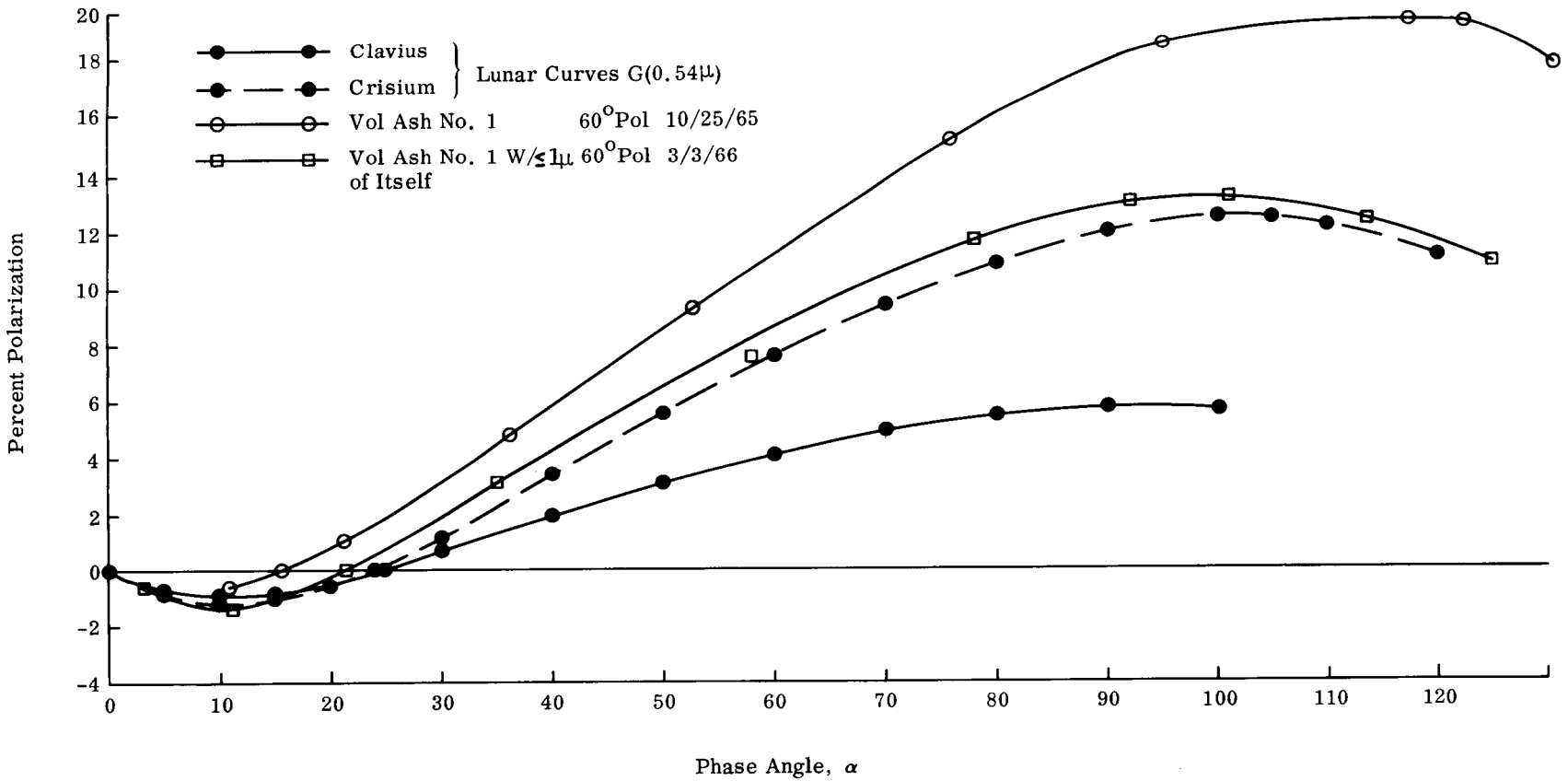

Fig. 8 Contrived Model No. 6 Development

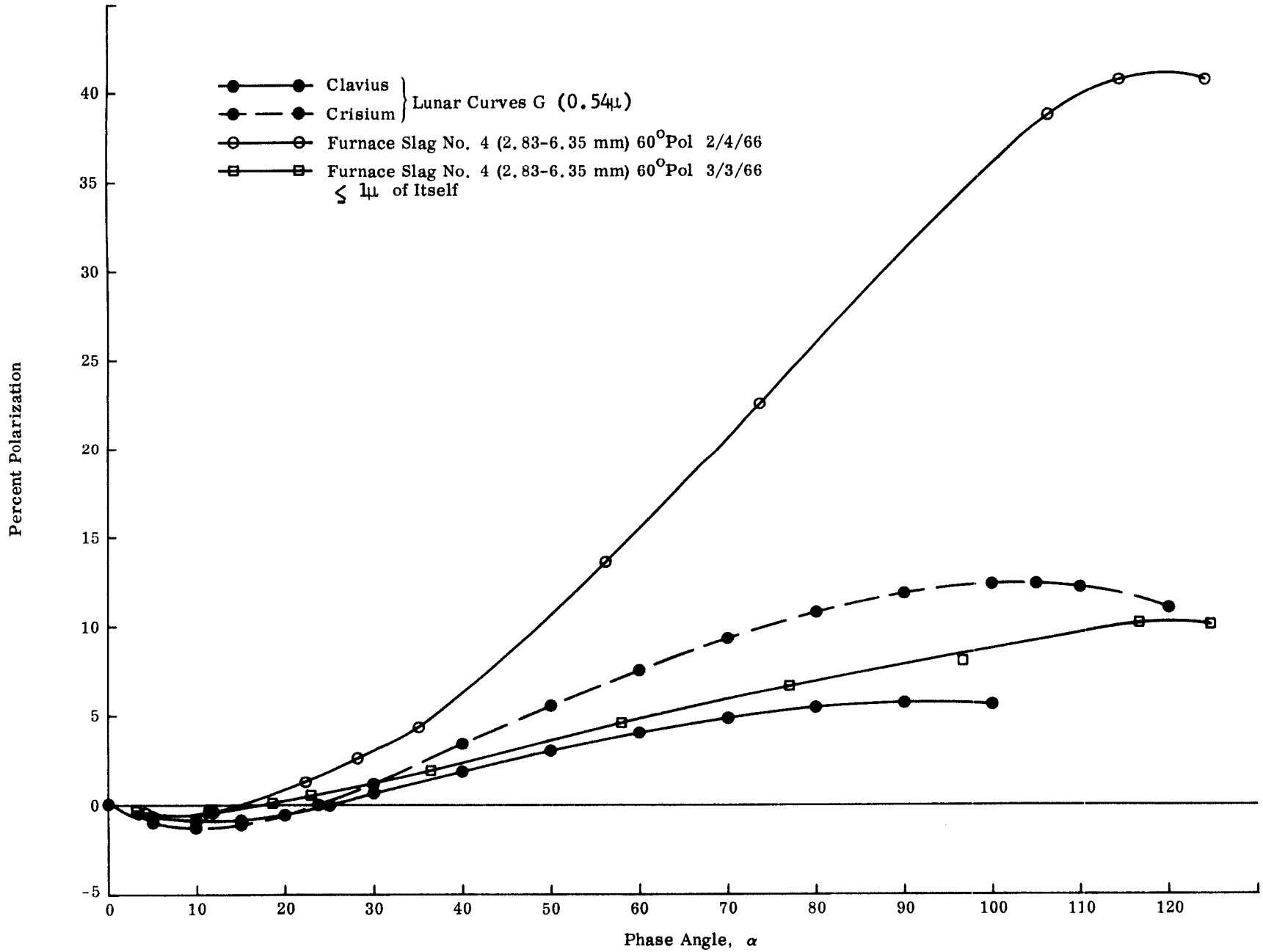

Fig. 9 Contrived Model No. 7 Development

a) Normal Incident Illumination

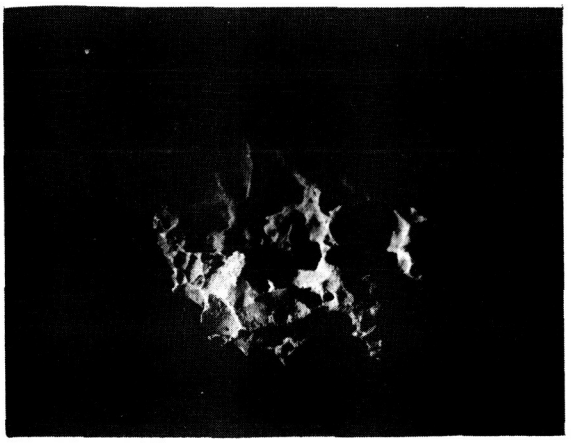

b) 65° Incident Illumination

Fig. 10 Contrived Model No. 1: Furnace Slag (Sponge Like-NASA) Topped with 0.088 to 0.21mm Particles of Volcanic Ash No. 1

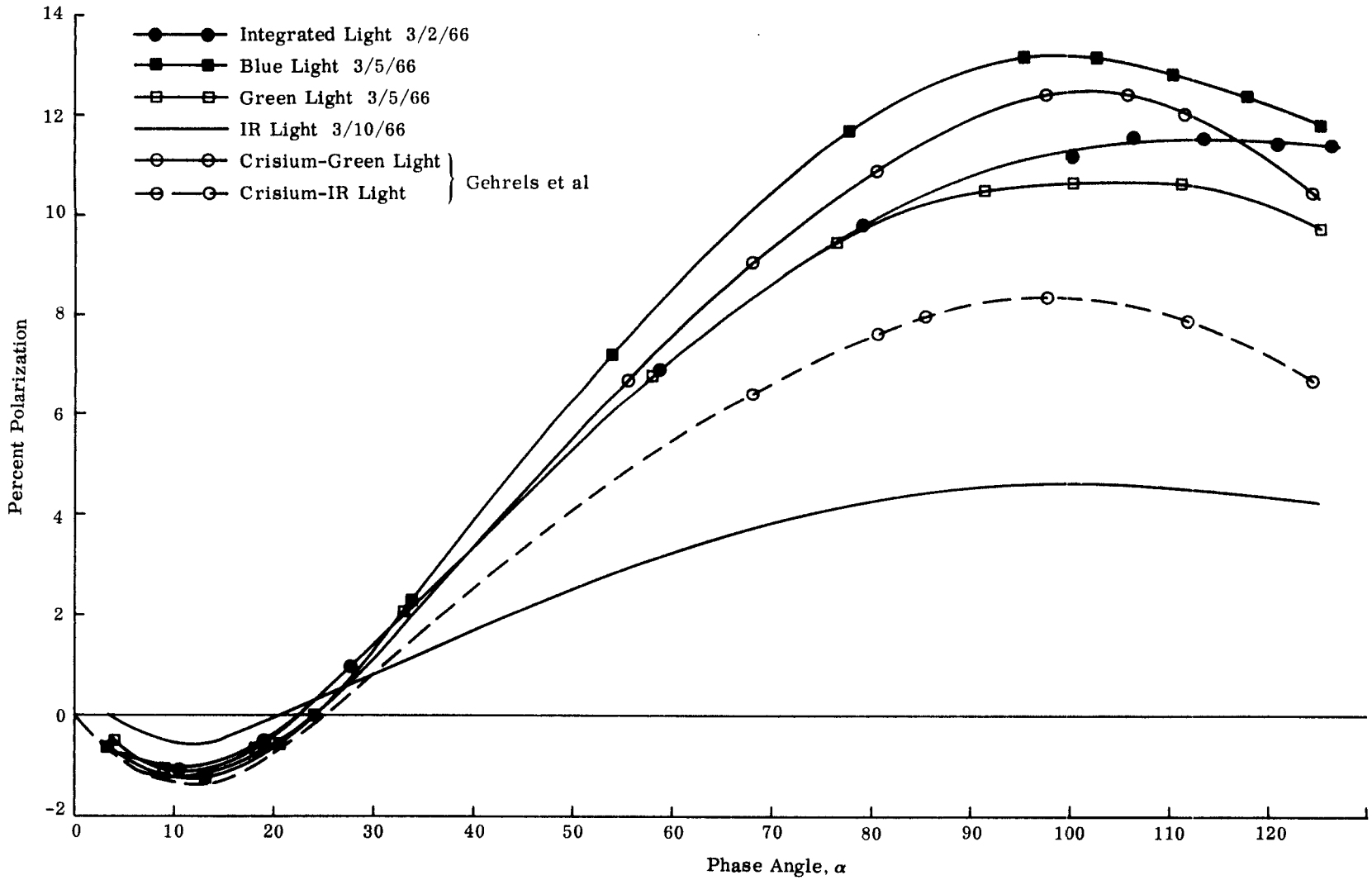

Fig. 11 Contrived Model No. 1: Percent Polarization as a Function of Color -- 60° Polarimeter

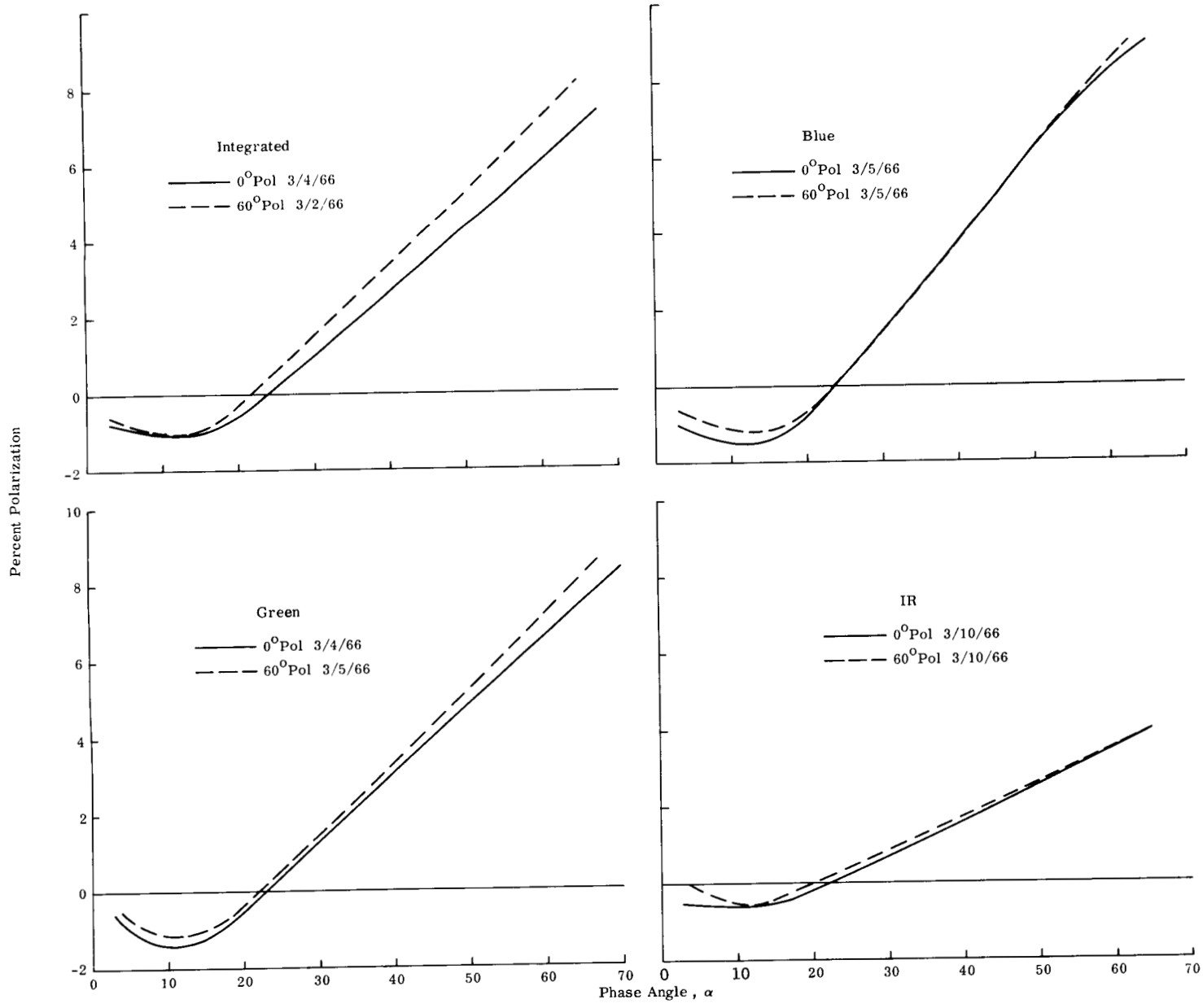

Fig. 12 Contrived Model No. 1: Simulated Lunar Longitude Effect on Percent Polarization as a Function of Color

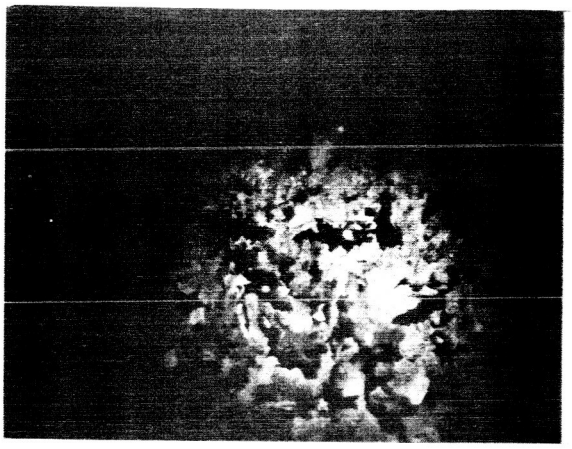

a) Normal Incident Illumination

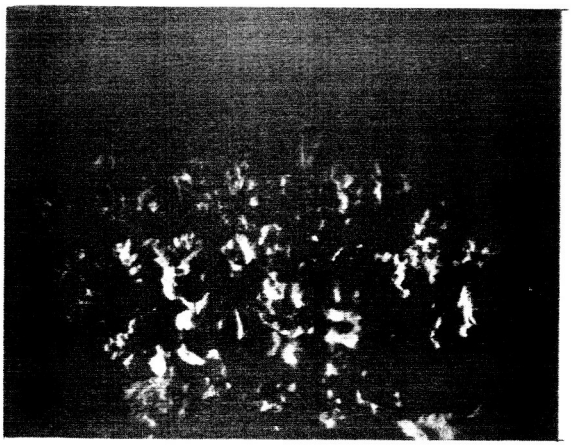

b) 65° Incident Illumination

Fig. 13 Contrived Model No. 2: Coral No. 1 Topped with Particles of Furnace Slag No. 4 $\leq$ 0.037mm

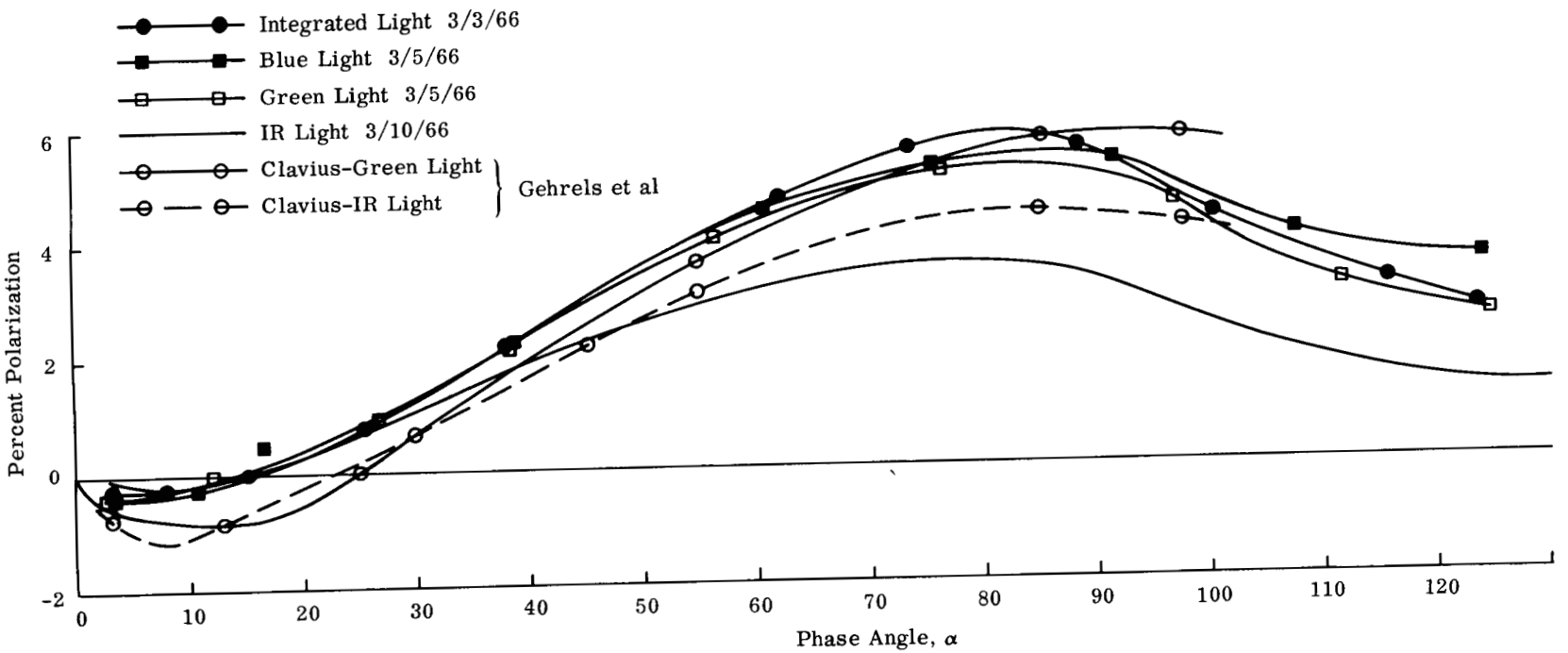

Fig. 14 Contrived Model No. 2: Percent Polarization as a Function of Color -- 60° Polarimeter

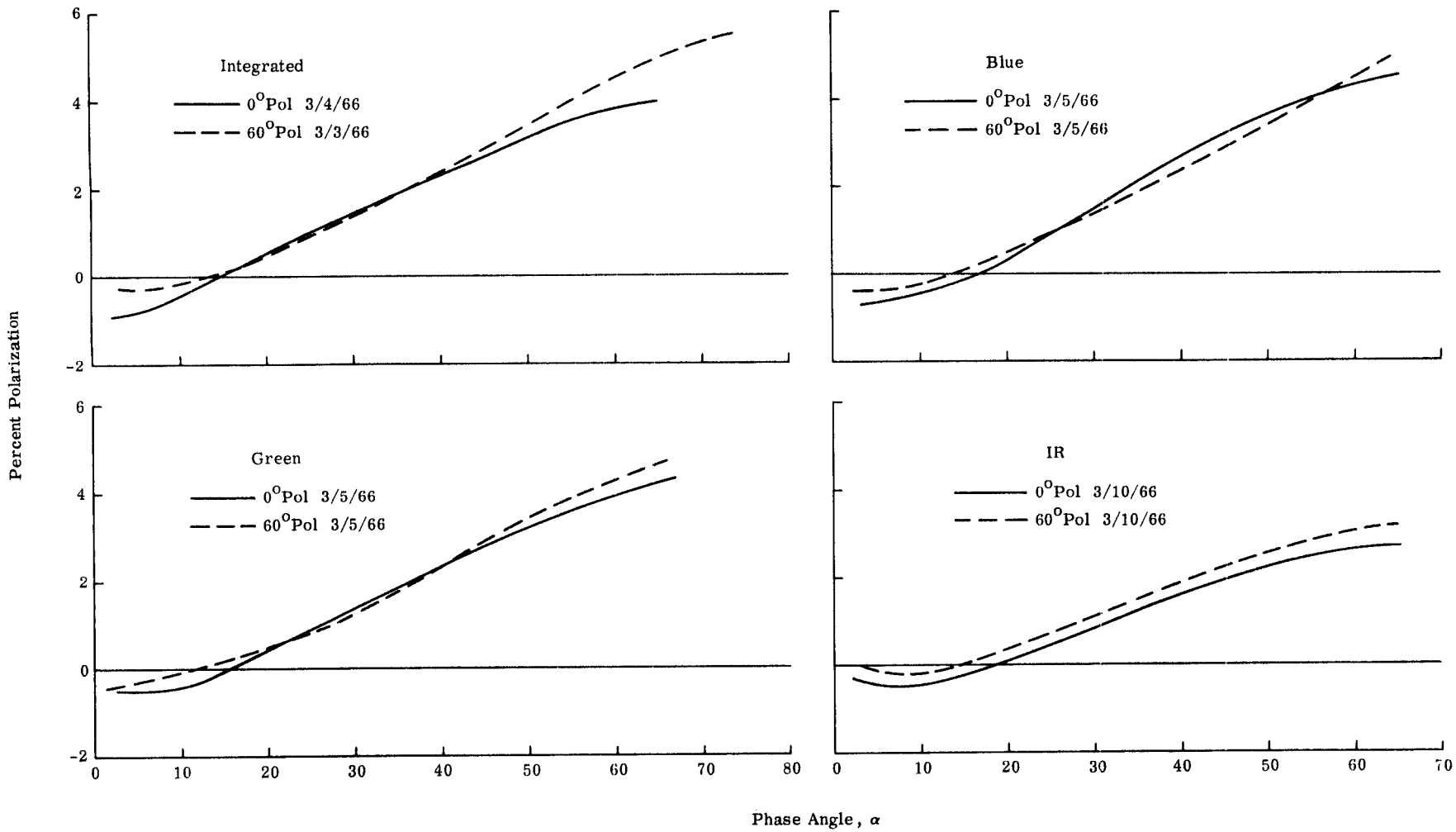

Fig. 15 Contrived Model No. 2: Simulated Lunar Longitude Effect on Percent Polarization as a Function of Color

a) Normal Incident Illumination

b) 65° Incident Illumination

Fig. 16 Contrived Model No. 4: Volcanic Ash No. 4 (chunks) Topped with Particles of Coral $\lesssim 1\mu$

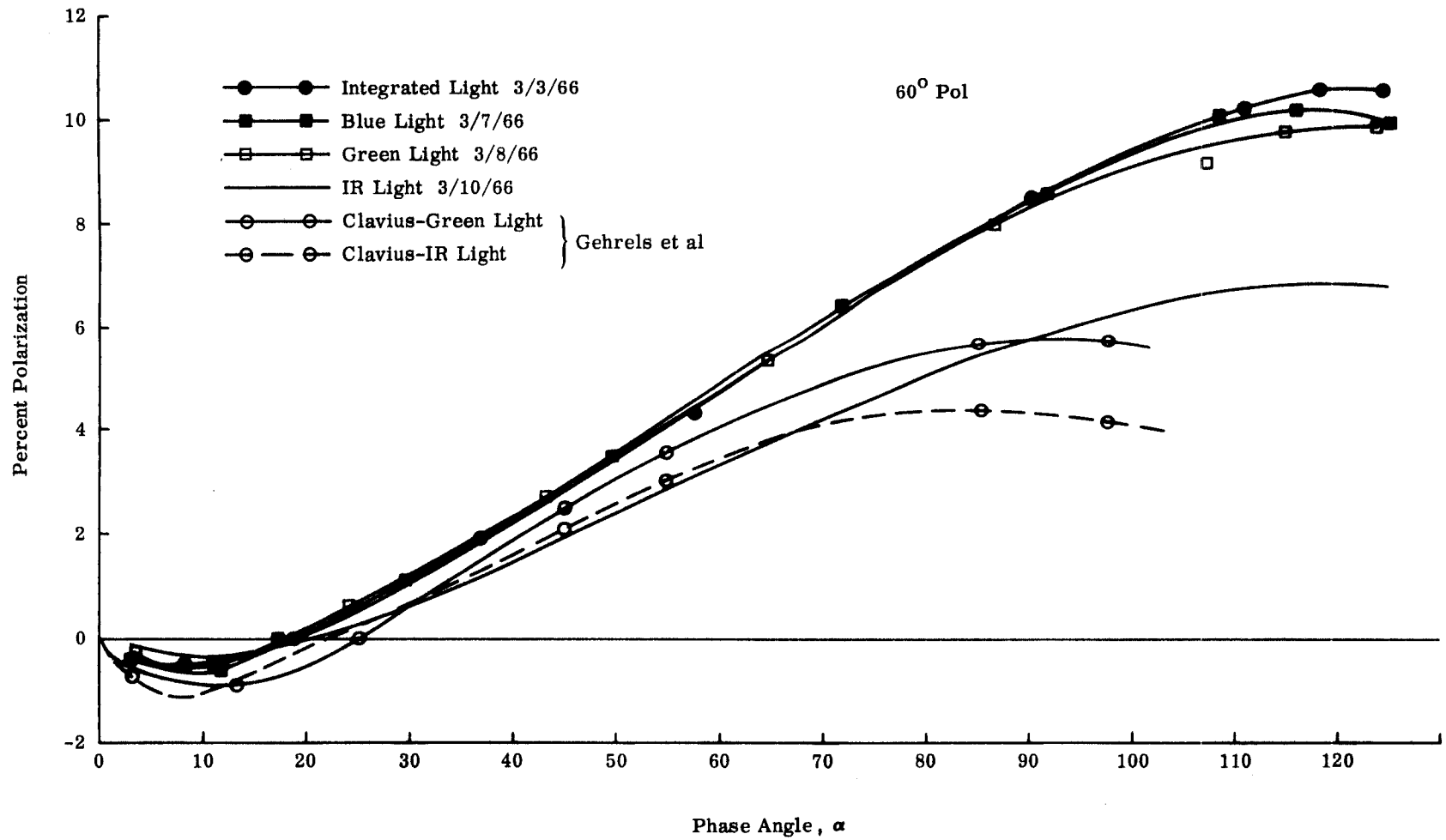

Fig. 17 Contrived Model No. 4: Percent Polarization as a Function of Color -- 60° Polarimeter

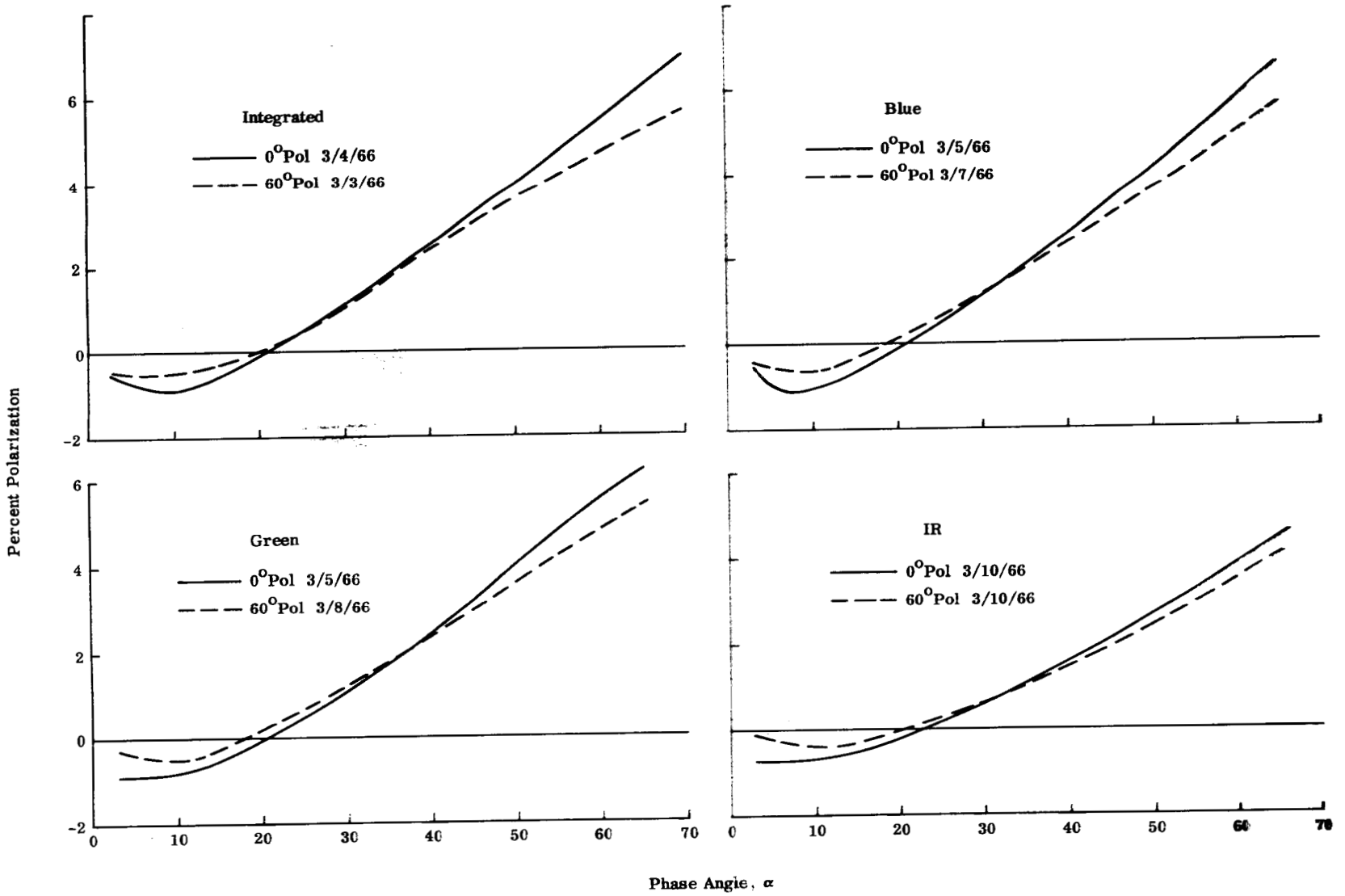

Fig. 18 Contrived Model No. 4: Simulated Lunar Longitude Effect on Percent Polarization as a Function of Color

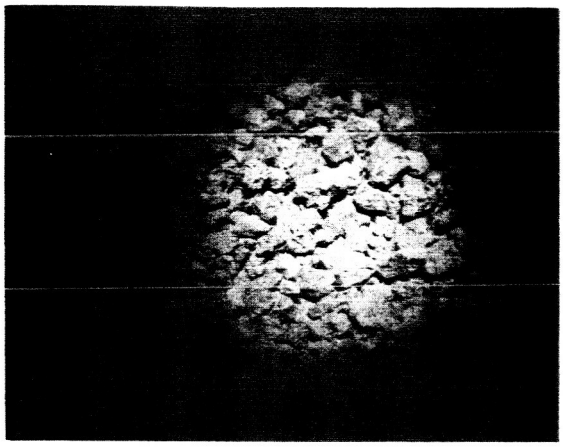

a) Normal Incident Illumination

b) 65° Incident Illumination

Fig. 19 Contrived Model No. 5: Volcanic Ash No. 4 Topped with Particles of Itself $\lesssim 1\mu$

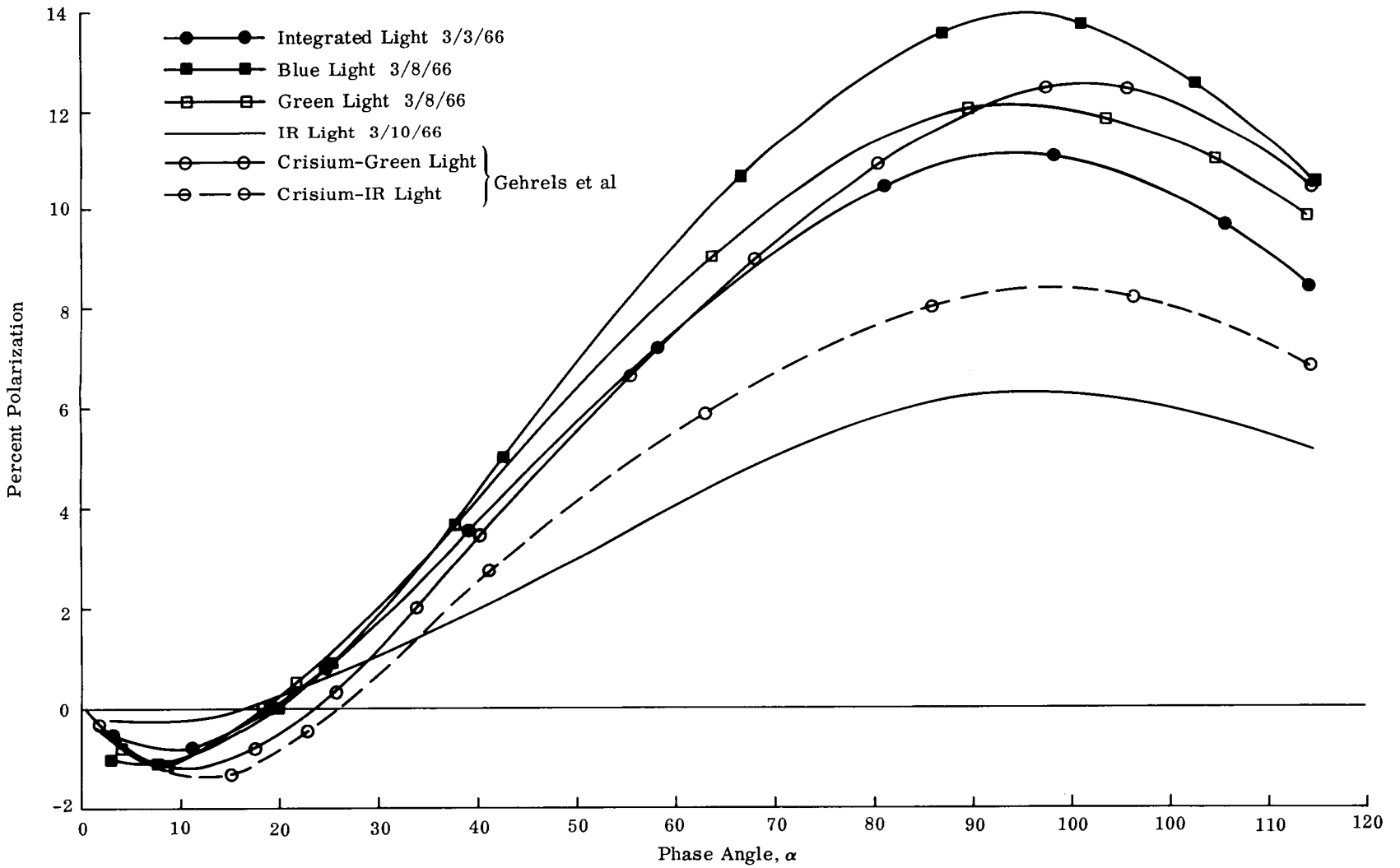

Fig. 20 Contrived Model No. 5: Percent Polarization as a Function of Color -- 60° Polarimeter

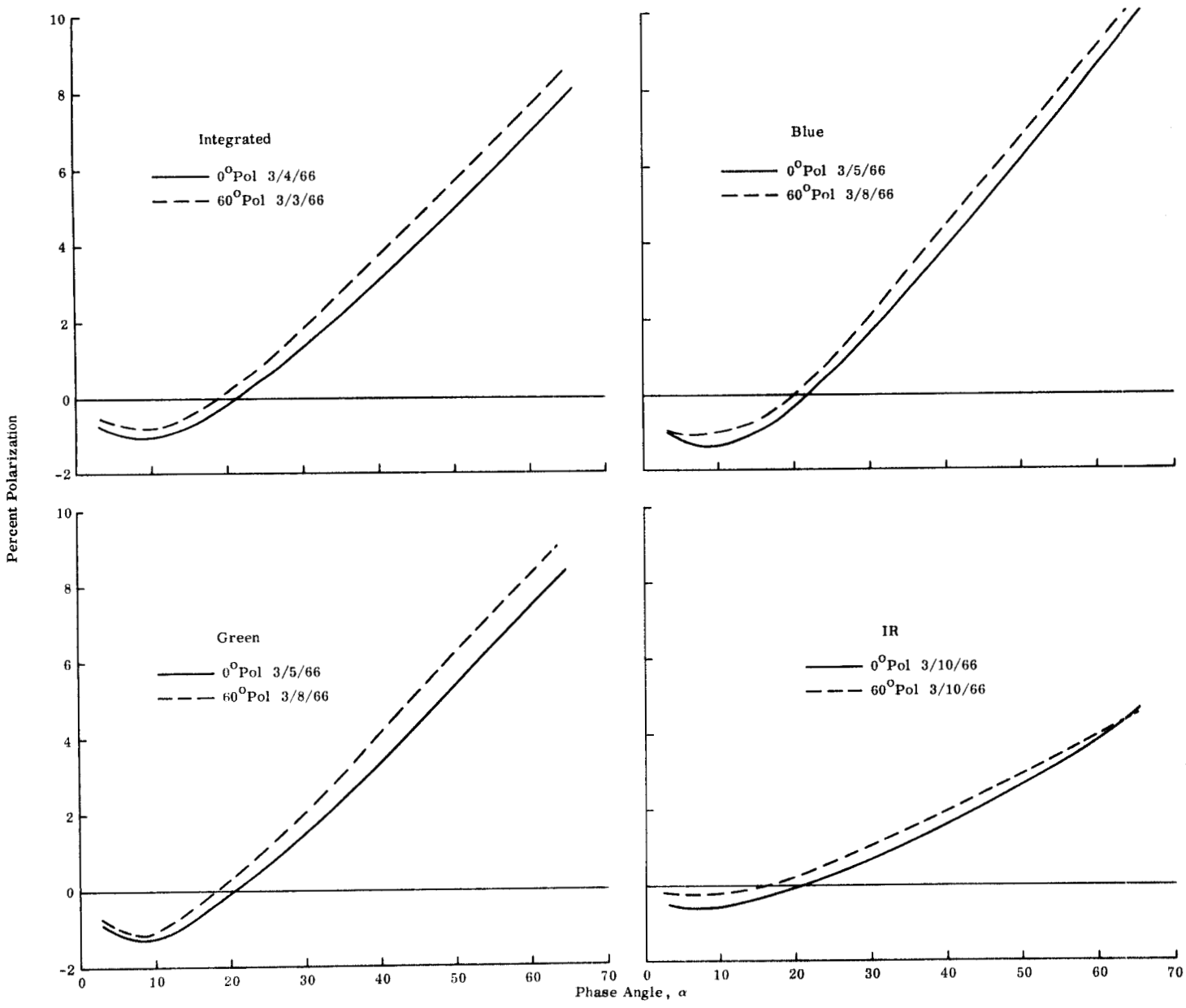

Fig. 21 Contrived Model No. 5: Simulated Lunar Longitude Effect on Percent Polarization as a Function of Color

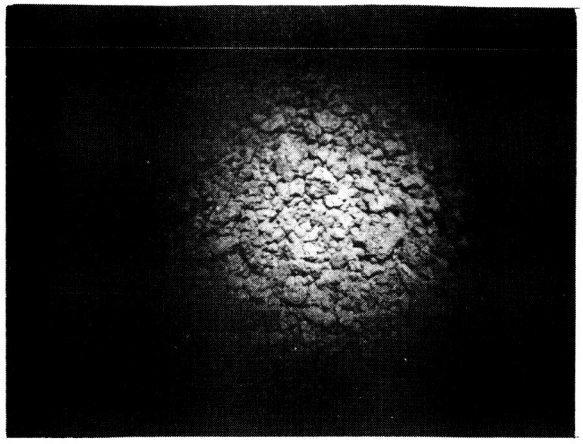

a) Normal Incident Illumination

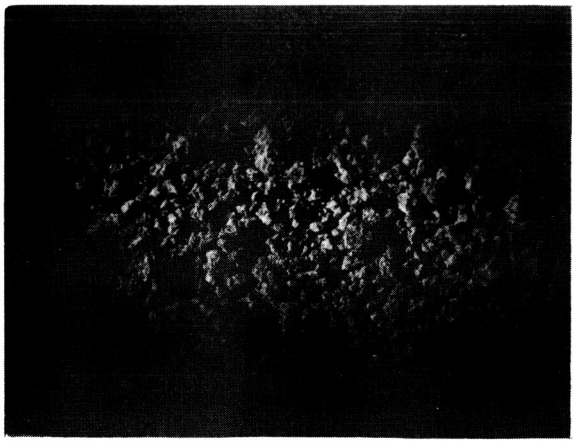

b) 65° Incident Illumination

Fig. 22 Contrived Model No. 6: Volcanic Ash No. 1 Topped with Particles of Itself $\lesssim 1\mu$

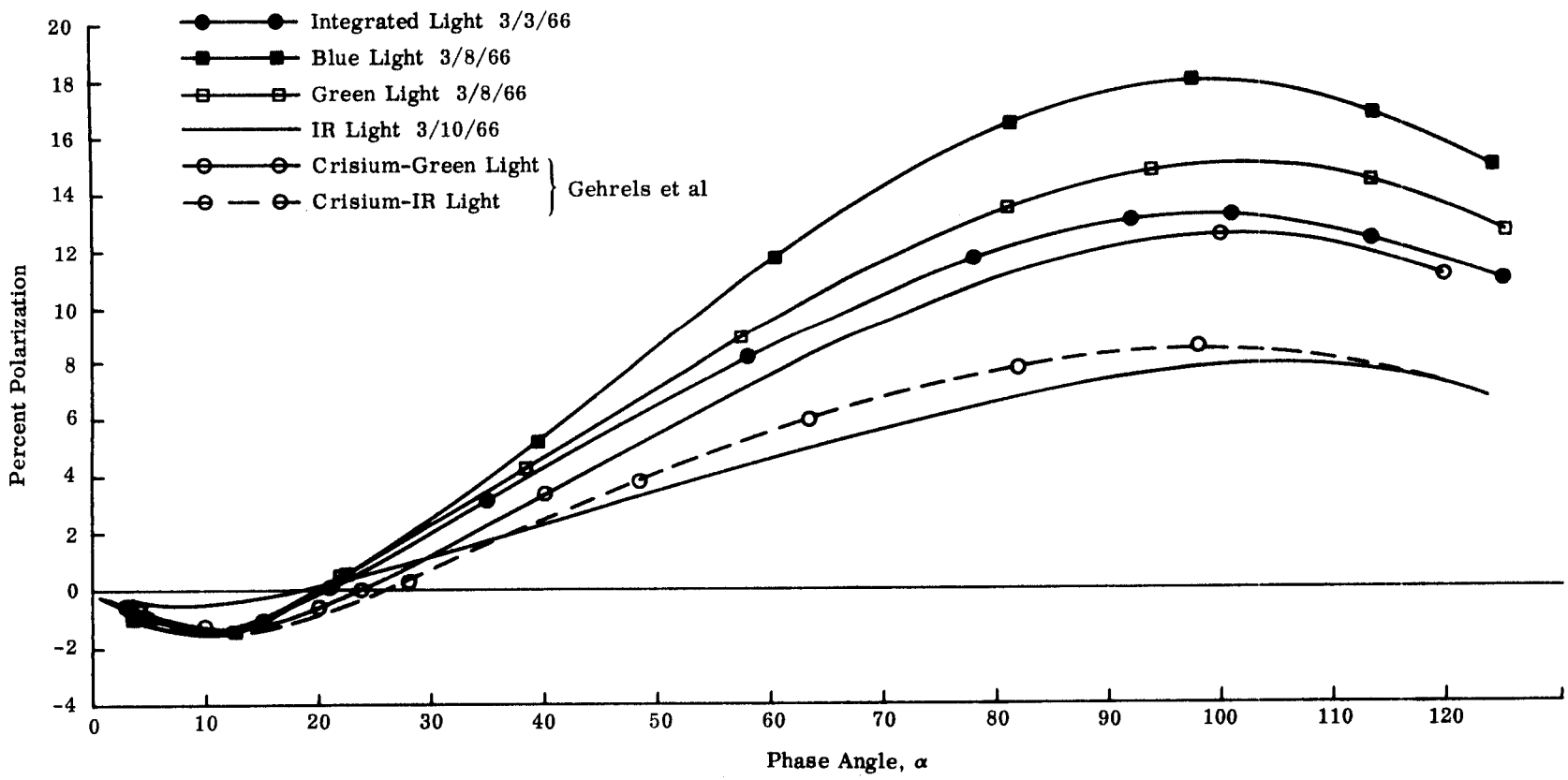

Fig. 23 Contrived Model No. 6: Percent Polarization as a Function of Color -- 60° Polarimeter

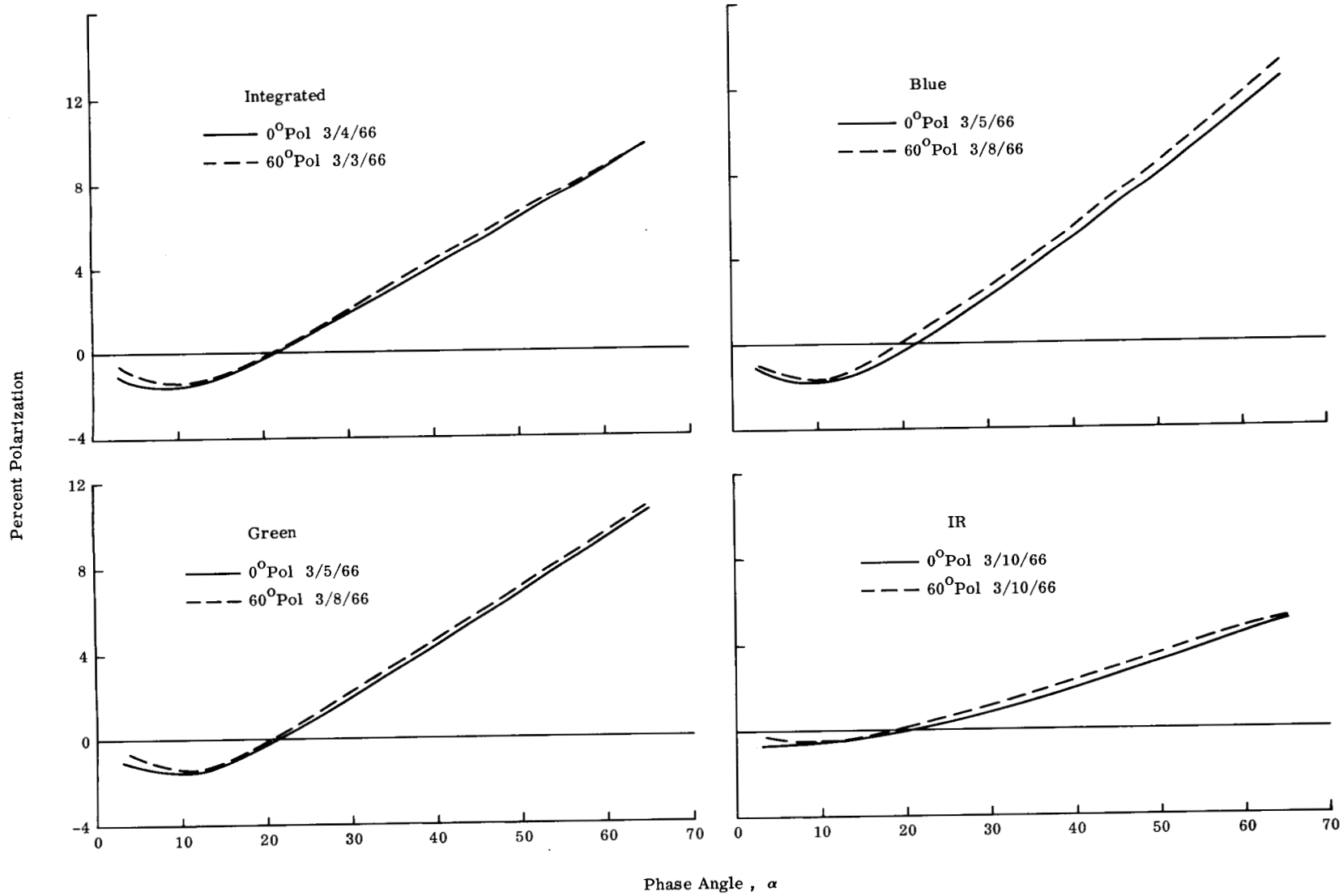

Fig. 24 Contrived Model No. 6: Simulated Lunar Longitude Effect on Percent Polarization as a Function of Color

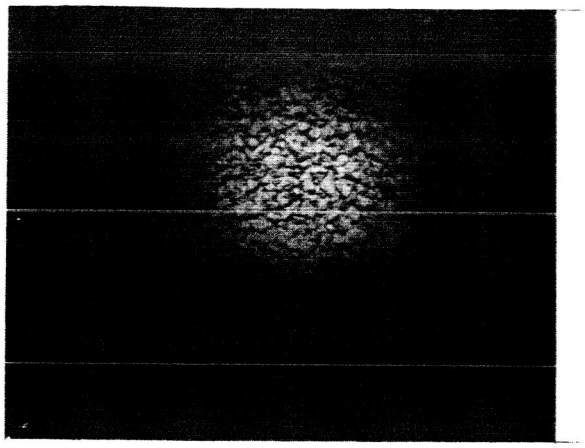

a) Normal Incident Illumination

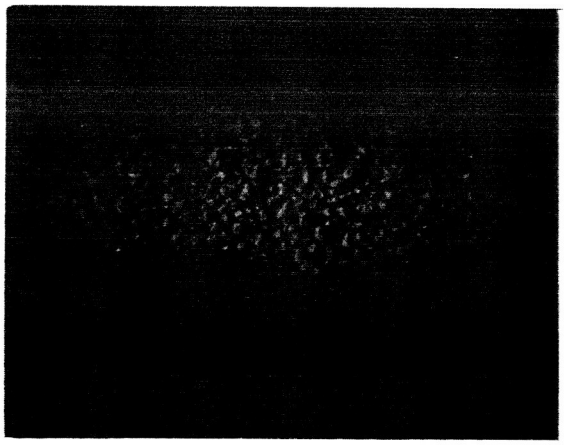

b) 65° Incident Illumination

Fig. 25 Contrived Model No. 7: Furnace Slag No. 4 Topped with Particles of Itself $\lesssim 1\mu$

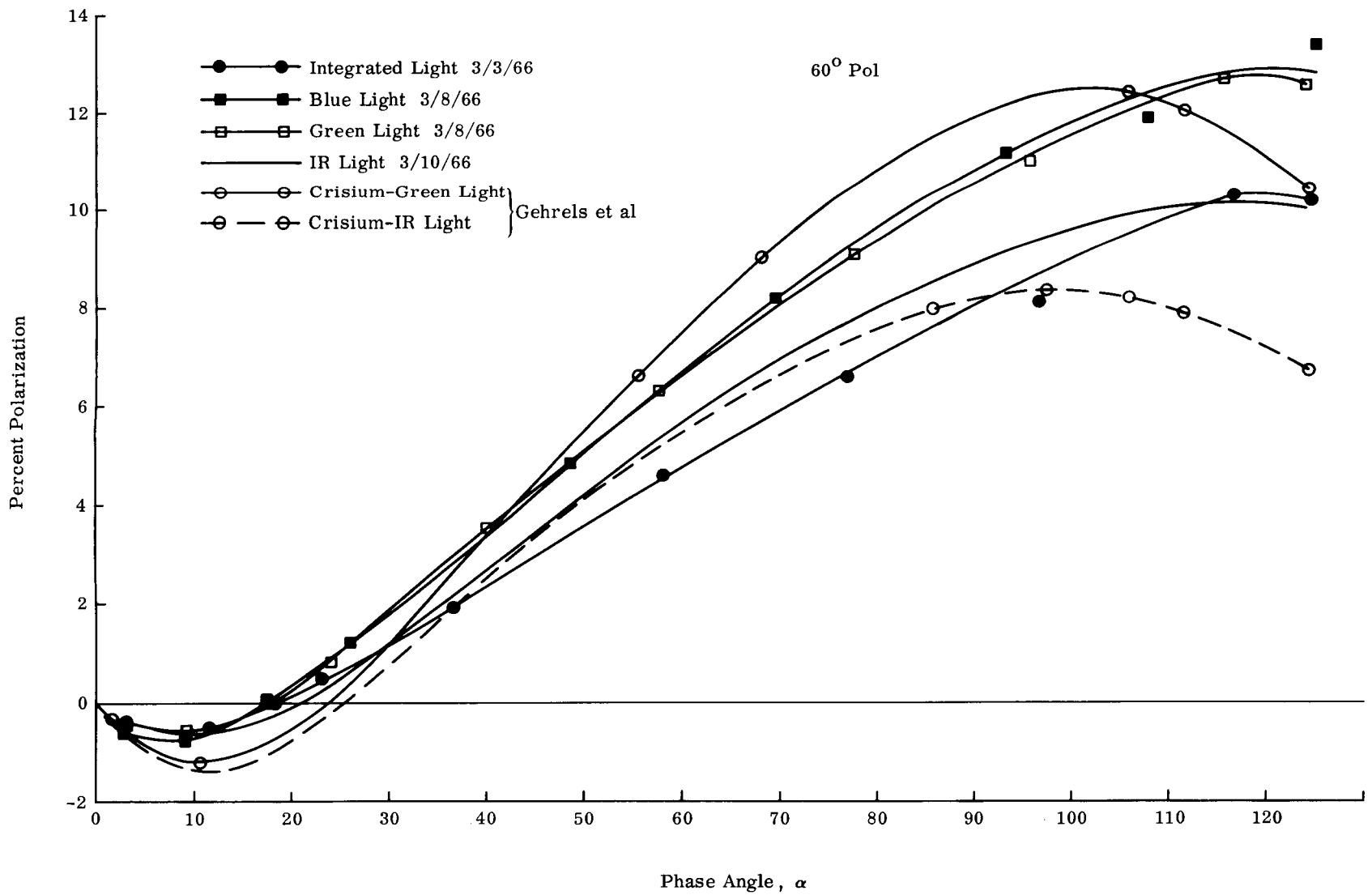

Fig. 26 Contrived Model No. 7: Percent Polarization as a Function of Color -- 60° Polarimeter

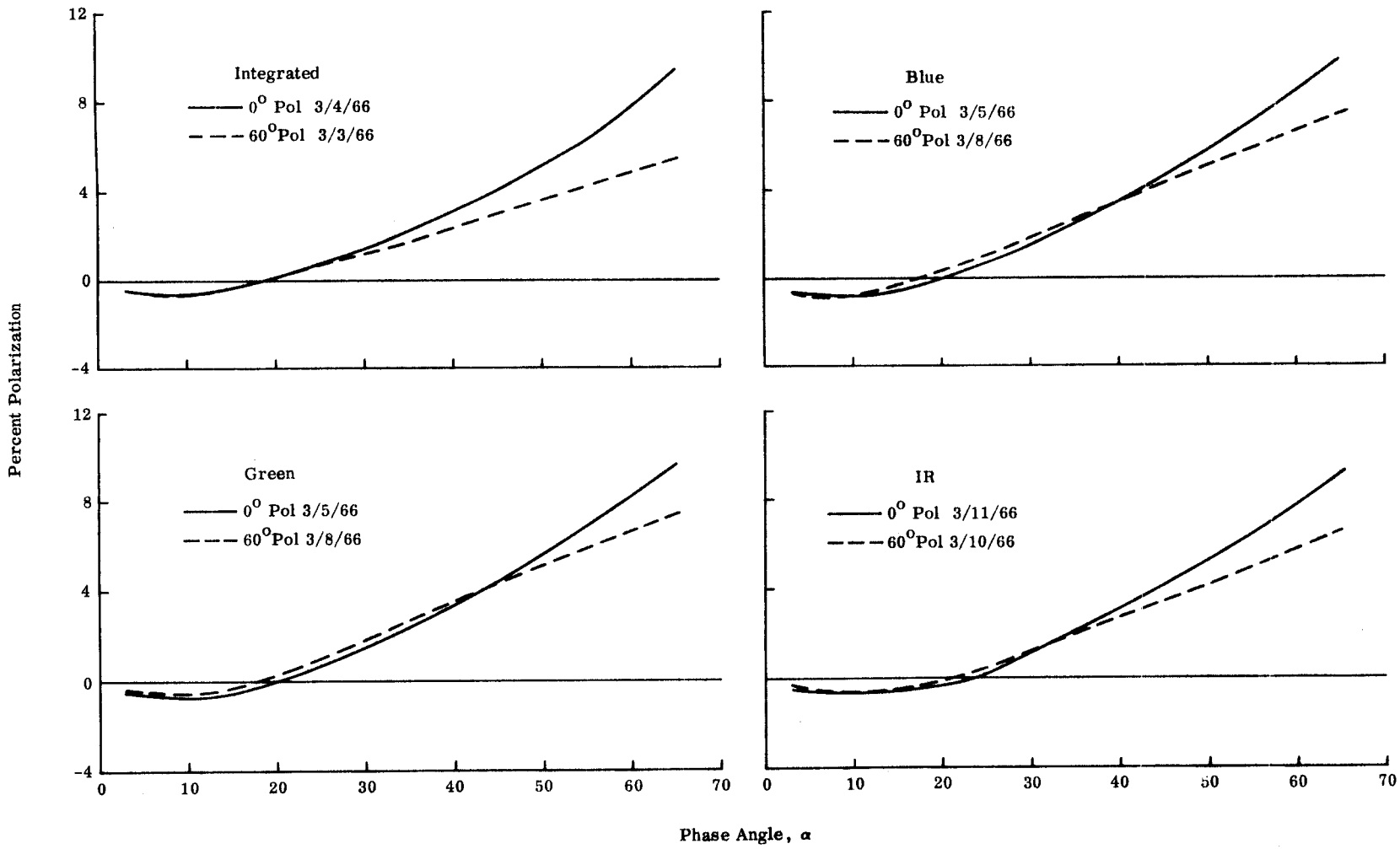

Fig. 27 Contrived Model No. 7: Simulated Lunar Longitude Effect on Percent Polarization as a Function of Color

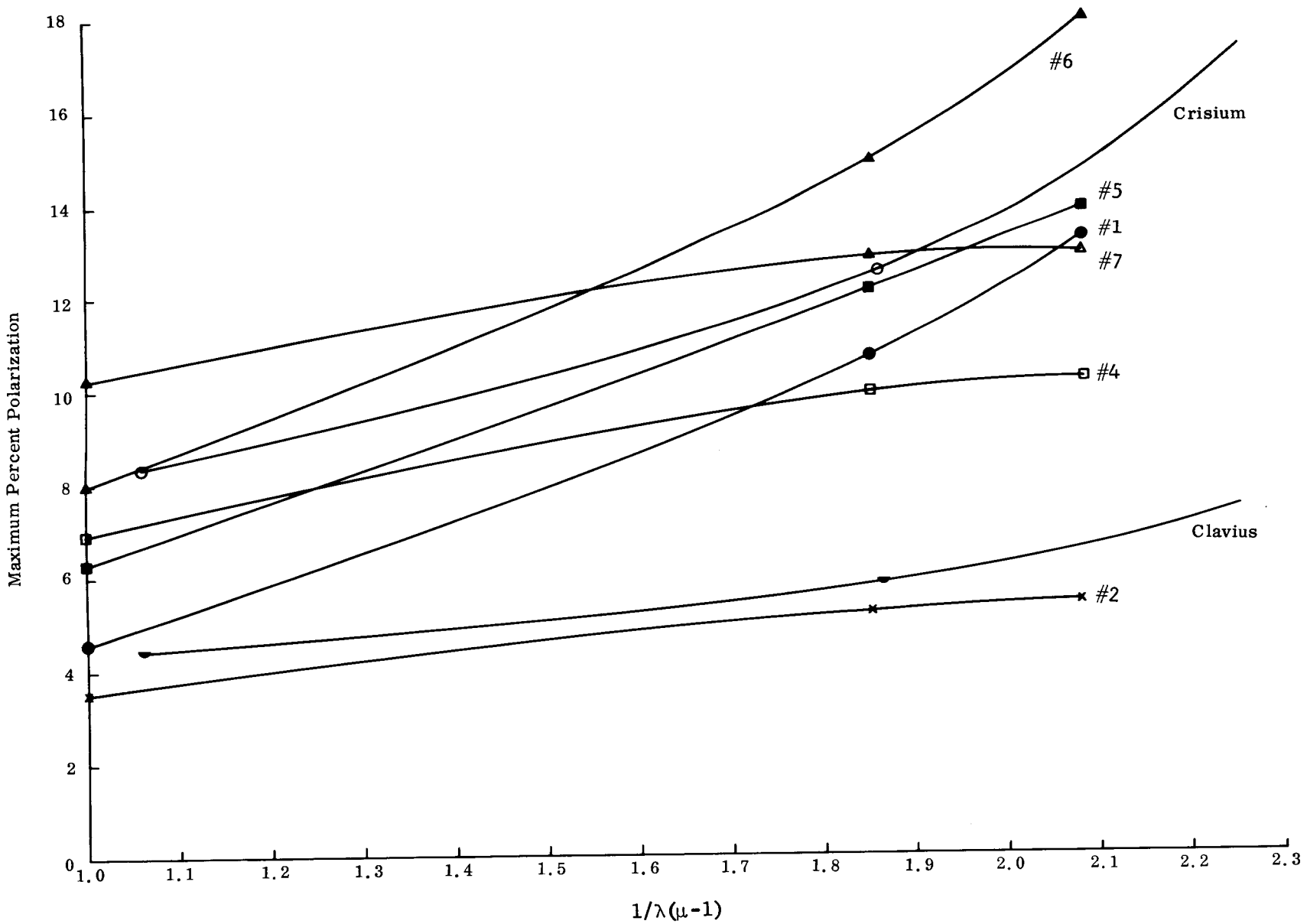

Fig. 28 Comparison of Maximum Percent Polarization as a Function of 1/λ

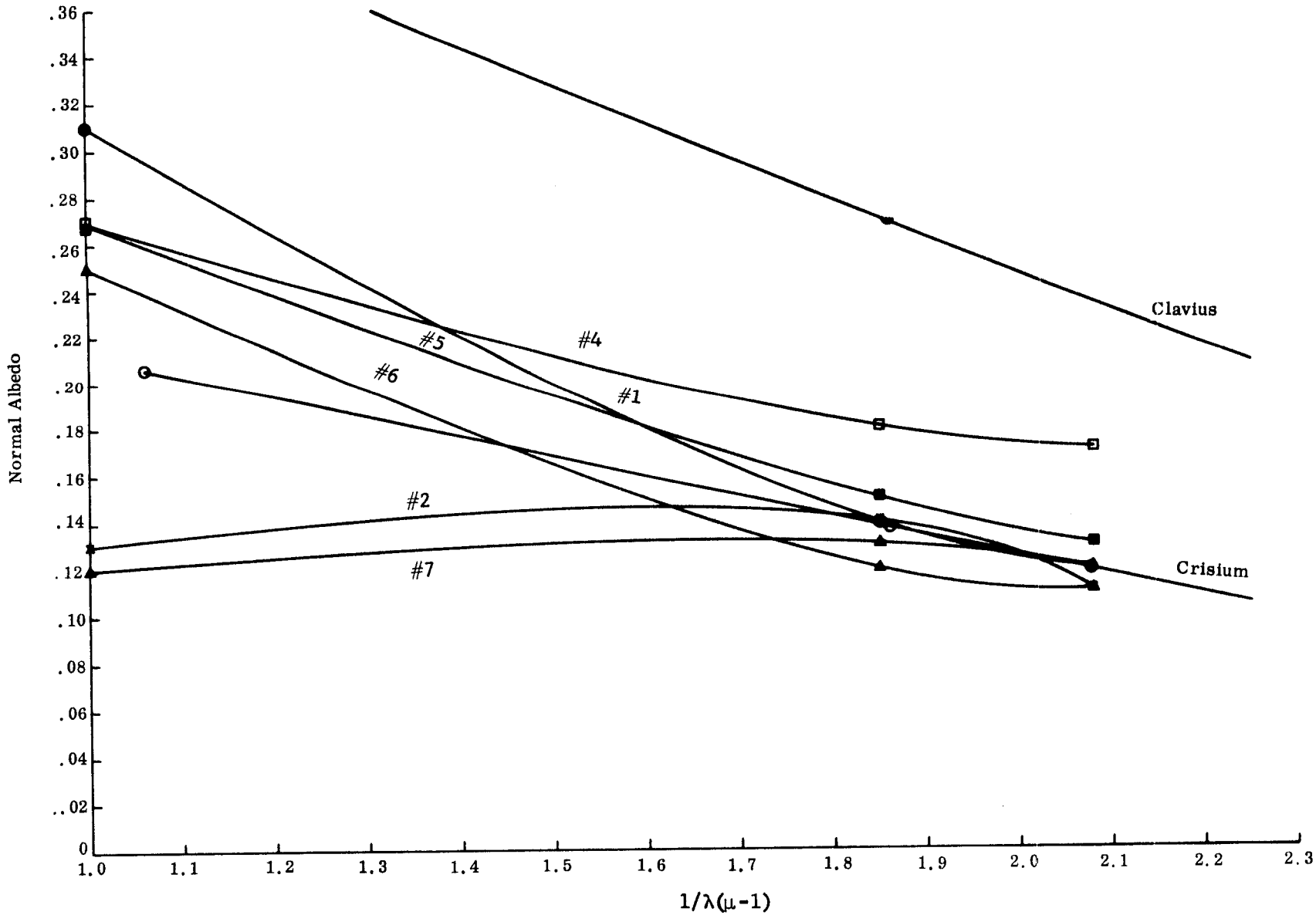

Fig. 29 Comparison of Normal Albedos as a Function of 1/λ

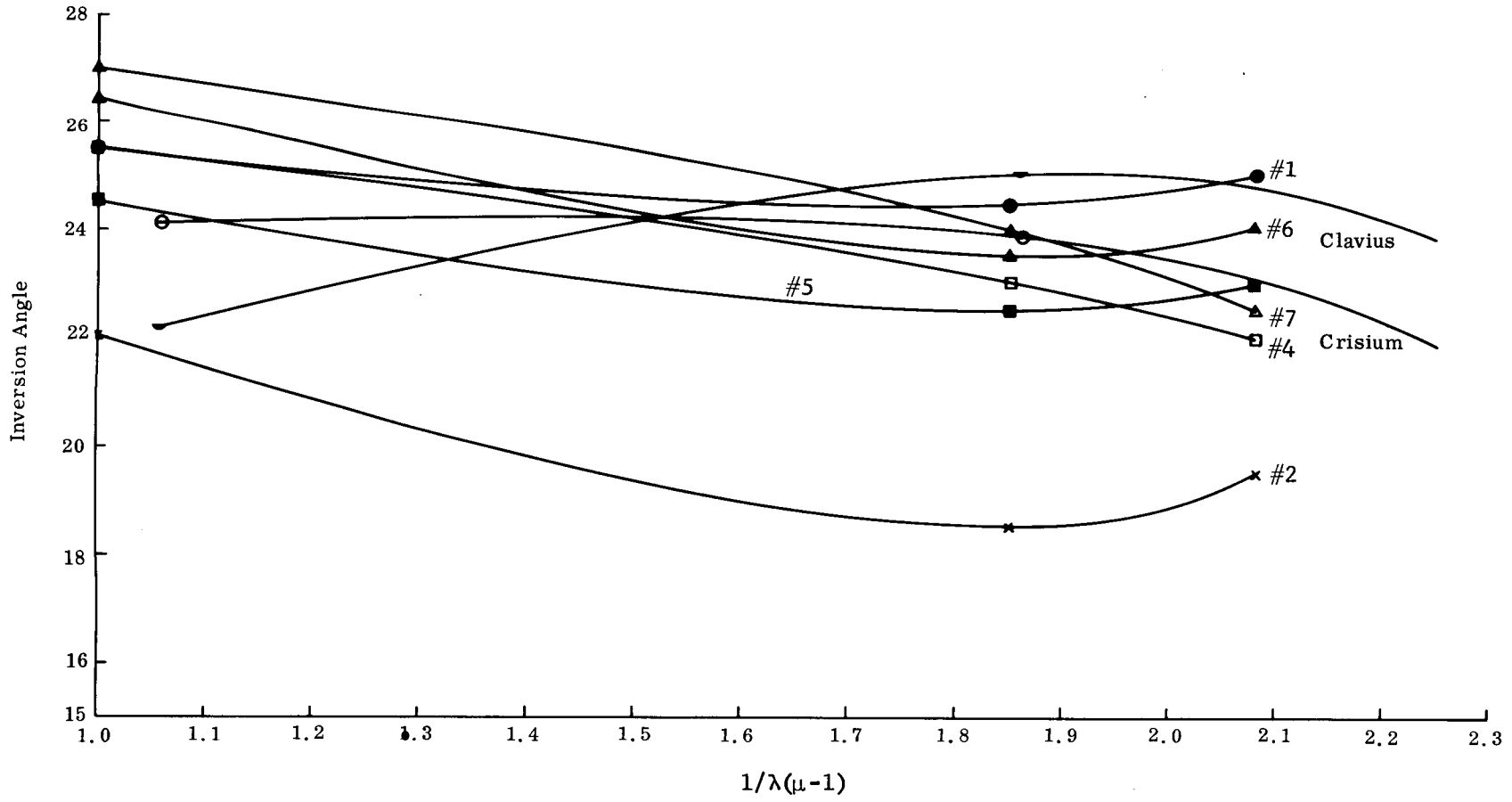

Fig. 30 Comparison of Inversion Angles as a Function of 1/λ

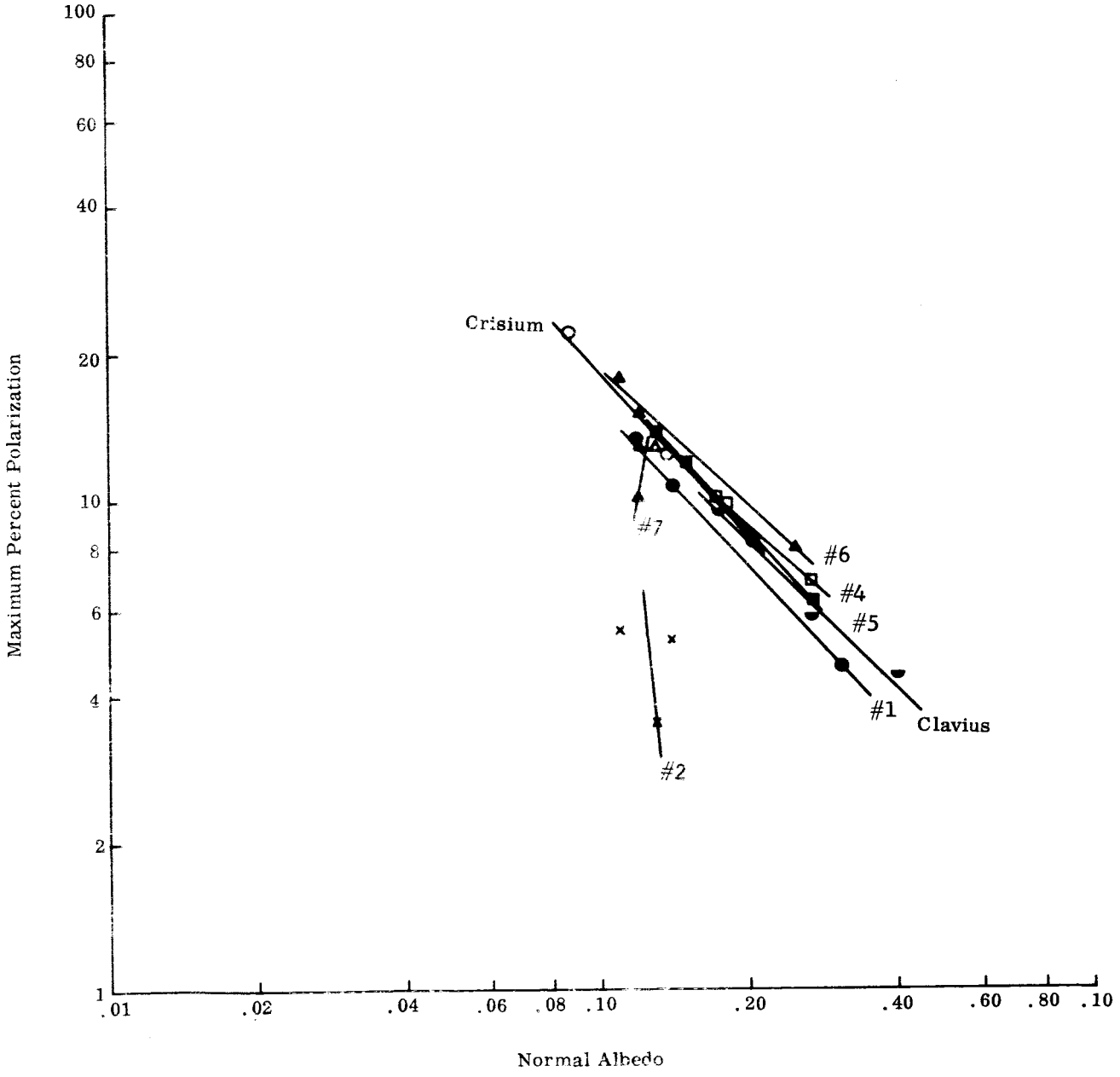

Fig. 31 Comparison of Maximum Percent Polarization as a Function of Albedo

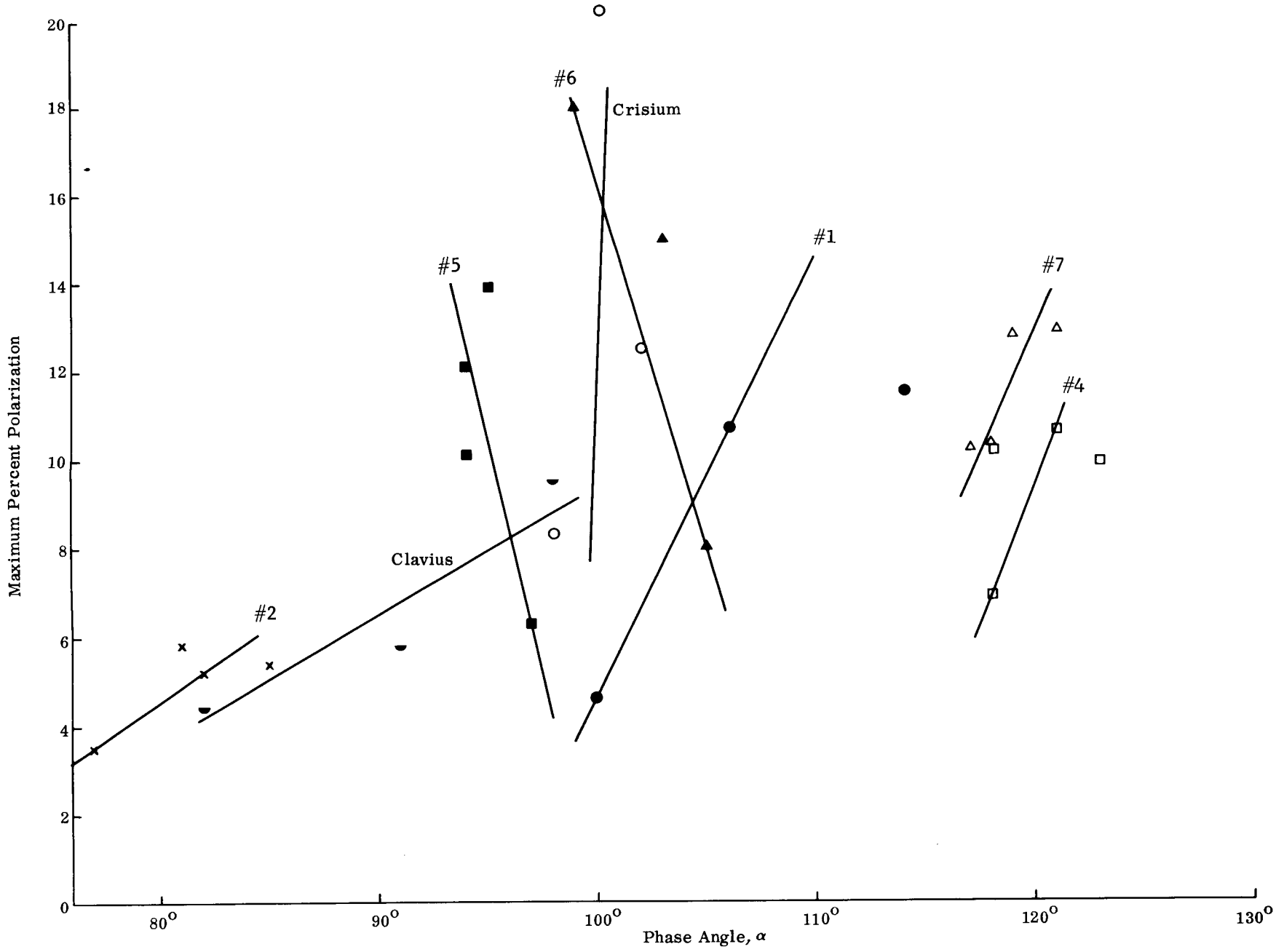

Fig. 32 Comparison of Maximum Percent Polarization and Corresponding Phase Angle

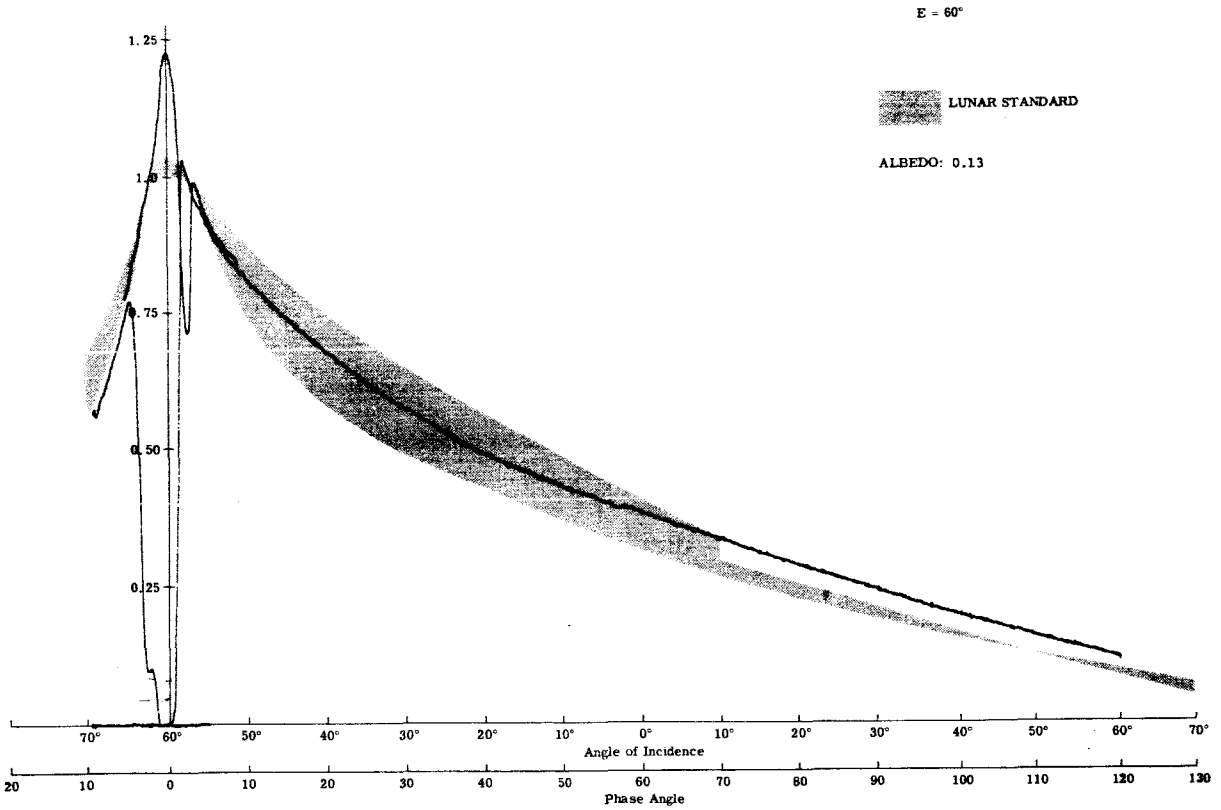

a) 60° Photometer-Visual Light

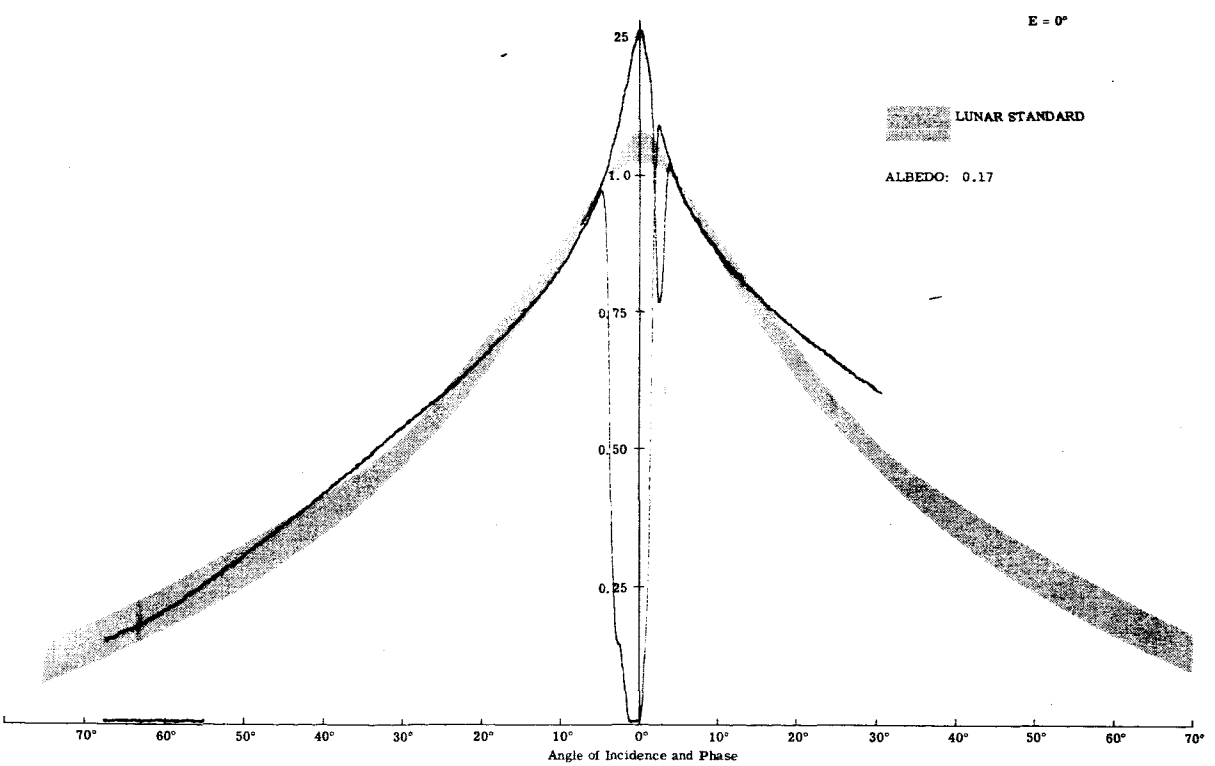

b) 0° Photometer-Visual Light

Fig. 33 Photometry of Contrived Model No. 1: Furnace Slag (Spongelike-NASA) Topped with 0.088 to 0.21 mm Particles of Volcanic Ash No. 1 (Brightness (Arbitrary Units) versus Phase Angle)

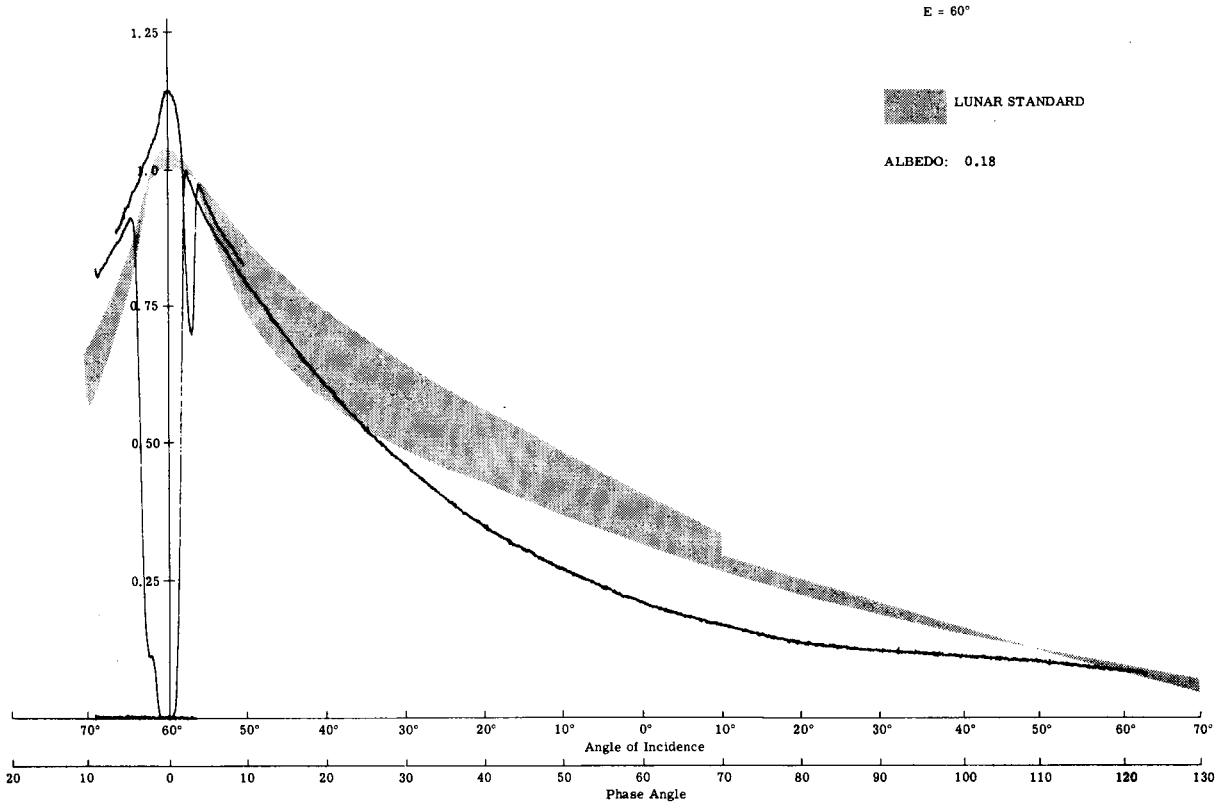

a) 60° Photometer-Visual Light

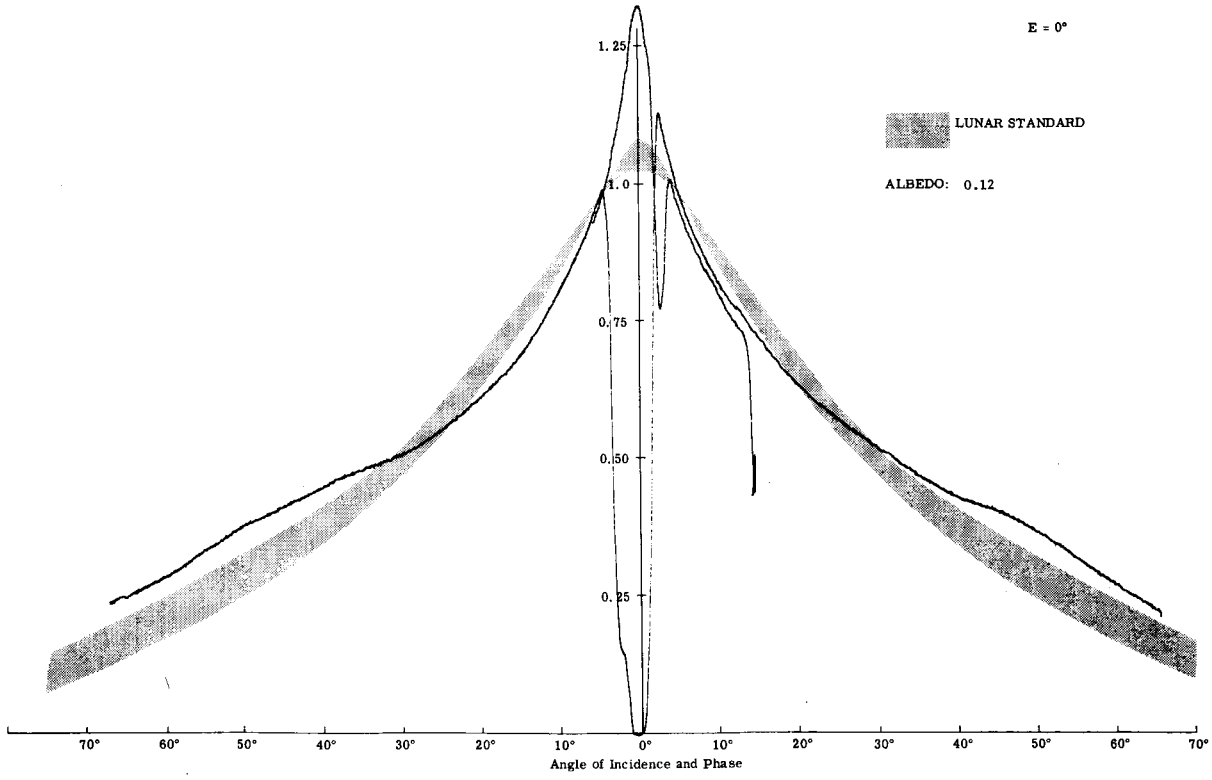

b) 0° Photometer-Visual Light

Fig. 34 Photometry of Contrived Model No. 2: Coral No. 1 Topped with Particles of Furnace Slag No. 4 $\lesssim$ 0.037 mm (Brightness (Arbitrary Units) versus Phase Angle)

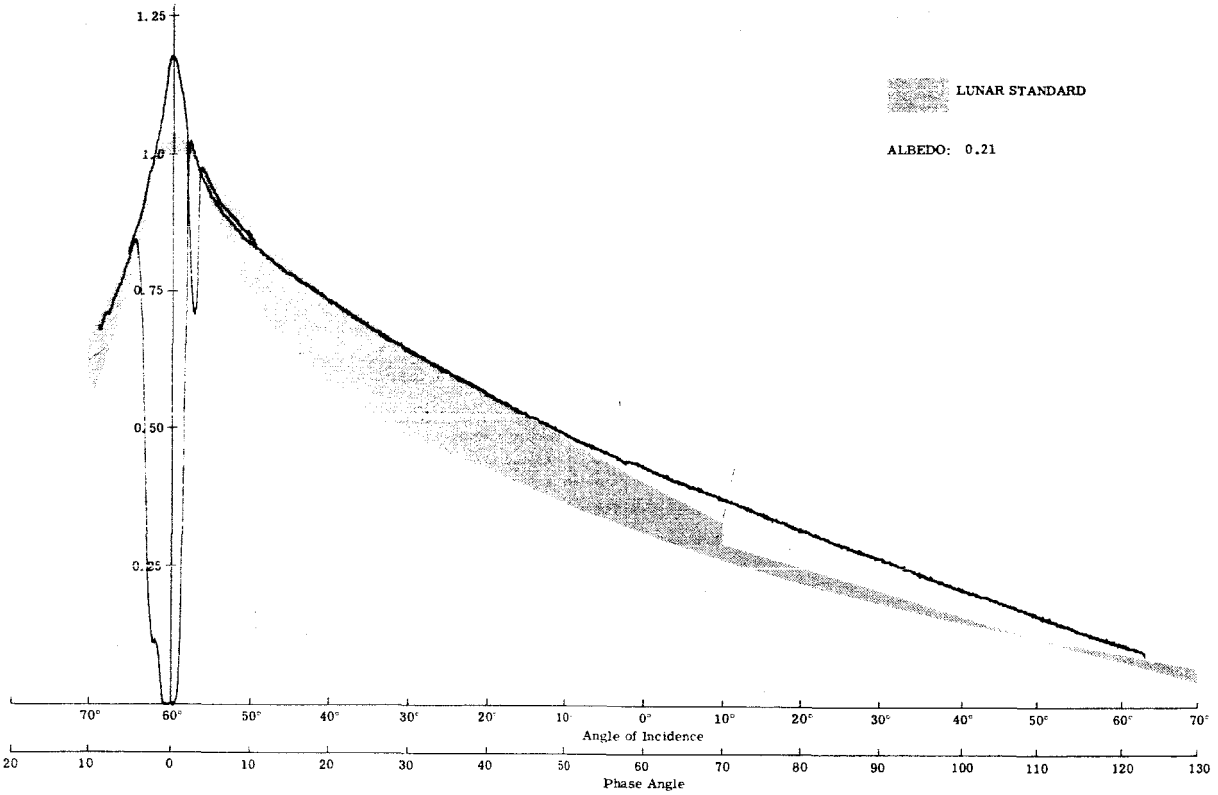

Fig. 35 Photometry of Contrived Model No. 4: Volcanic Ash No. 4 (Chunks) Topped with Particles of Coral $\leq 1\mu$ -- 60° Photometer-Visual Light (Brightness (Arbitrary Units) versus Phase Angle)

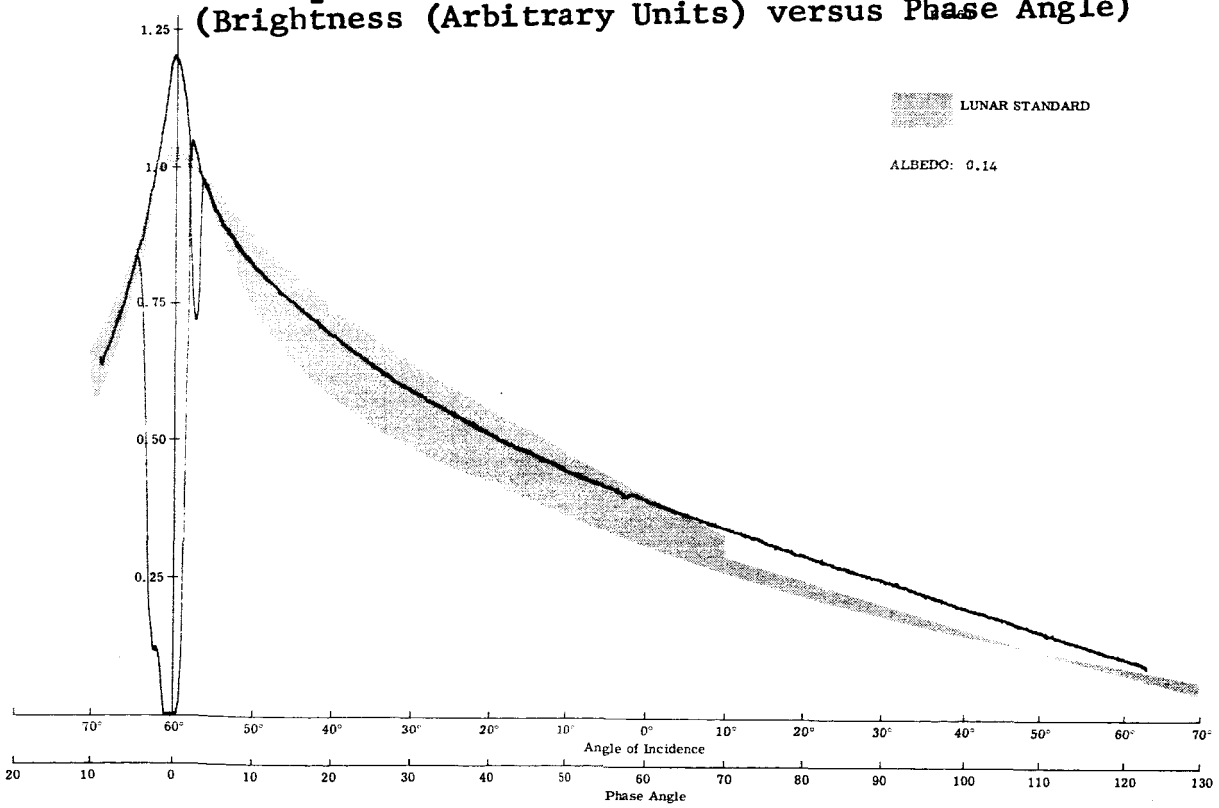

Fig. 36 Photometry of Co trived Model No. 5: Volcanic Ash No. 4 Topped with Particles of Itself $\leq 1\mu$ (Brightness (Arbitrary Units) versus Phase Angle)

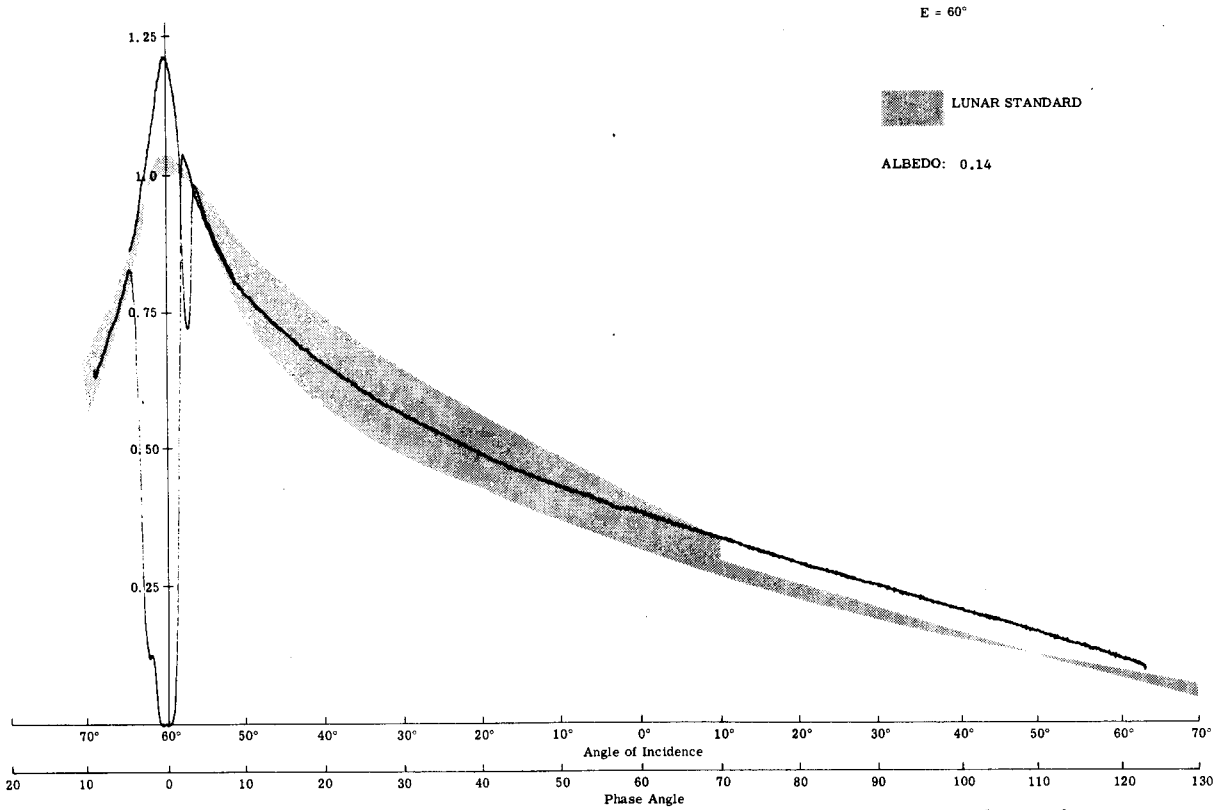

Fig. 37 Photometry of Contrived Model No. 6: Volcanic Ash No. 1 Topped with Particles of Itself $\lesssim 1\mu$ (Brightness (Arbitrary Units) versus Phase Angle)

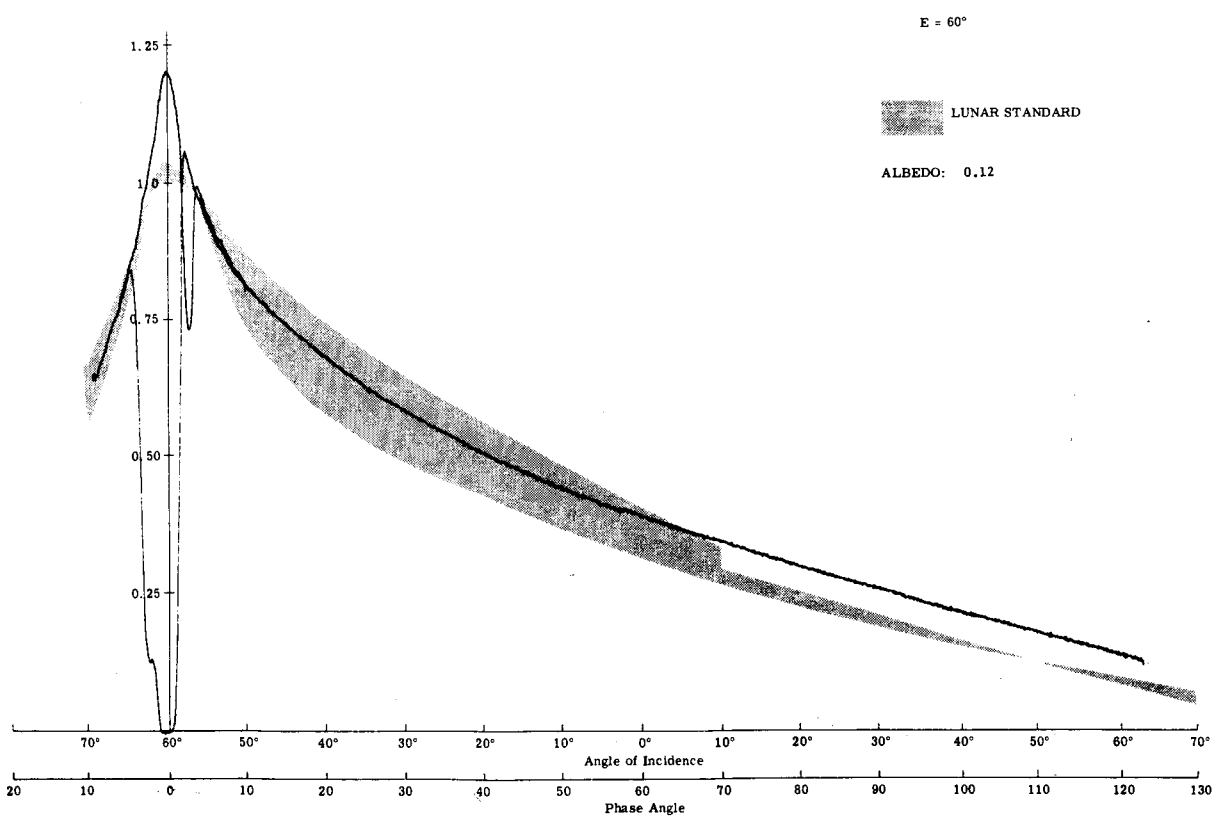

Fig. 38 Photometry of Contrived Model No. 7: Furnace Slag No. 4 Topped with Particles of Itself $\lesssim 1\mu$ (Brightness (Arbitrary Units) versus Phase Angle)